Black mamba venom peptides target acid-sensing ion channels to abolish pain

Sylvie Diochot, Anne Baron, Miguel Salinas, Dominique Douguet, Sabine Scarzello, Anne-Sophie Dabert-Gay, Delphine Debayle, Valérie Friend, Abdelkrim Alloui, Michel Lazdunski, et al.

Black mamba venom peptides target Acid-Sensing Ion channels to abolish pain

Sylvie Diochot*[1,2,3], Anne Baron*[1,2,3], Miguel Salinas[1,2,3], Dominique Douguet[1,2], Sabine Scarzello[1,2,4], Anne-Sophie Dabert-Gay[1,2], Delphine Debayle[1,2], Valérie Friend[1,2,3], Abdelkrim Alloui[5,6], Michel Lazdunski[1,2], Eric Lingueglia[1,2,3]

[1]: CNRS, Institut de Pharmacologie Moléculaire et Cellulaire, UMR 7275, 06560 Valbonne, France
[2]: Université de Nice-Sophia Antipolis, 06560 Valbonne, France
[3]: LabEx Ion Channel Science and Therapeutics, 06560 Valbonne, France.
[4]: present address : IRCAN, CNRS UMR 7284, Inserm U1081, UNS, 06107 Nice, France.
[5]: Clermont Université, Université d'Auvergne, NEURO-DOL, BP 10448, F-63000 Clermont-Ferrand, France.
[6] : Inserm U1107, F-63001 Clermont-Ferrand, France.
*: These authors contributed equally to this work

Polypeptide toxins have played a central role in understanding physiological and physiopathological functions of ion channels[1, 2]. In the field of pain, they led to significant advances in basic research[3-6] and even to clinical applications[7, 8]. Acid-Sensing Ion Channels (ASICs) are generally considered as major players in the pain pathway[9], including in human[10]. A snake toxin activating peripheral ASICs in nociceptive neurons has been recently shown to evoke pain[11]. Here we show that a new class of three-finger peptides from another snake, the black mamba, is able to abolish pain through inhibition of particular subtypes of ASIC channels expressed either in central or peripheral neurons. These peptides, which have been called mambalgins, are not toxic in mice but display a potent analgesic activity upon central and peripheral injection that can be as strong as morphine but resistant to naloxone, with much less tolerance and no respiratory distress. Pharmacological inhibition by mambalgins combined with the use of knockdown and knockout animals indicates the important involvement in pain perception of heteromeric channels made of ASIC1a and ASIC2a subunits in central neurons and of ASIC1b-containing channels in nociceptors. These findings identify new potential therapeutic targets for pain and introduce natural peptides that block them to produce a potent analgesia.

In a screen to discover new blockers of ASIC channels from animal venoms, we identified the venom of black mamba (*Dendroaspis polylepis polylepis*) as a potent and reversible inhibitor of the ASIC1a channel expressed in *Xenopus* oocytes (**Fig. 1a**). After purification, two active fractions were collected (**Supplementary Fig.1a,b**). A partial amino-acid sequence was used to clone by degenerated PCR the corresponding cDNA from lyophilized venom (**Supplementary Fig. 1c**). Two isopeptides were identified and named mambalgin-1 and mambalgin-2. They are composed of 57 amino acids with 8 cysteine residues, and only differ by one residue at position 4 (**Supplementary Fig. 1d**).
Mambalgins belong to the family of three-finger toxins[12] (**Supplementary Fig. 1d,e**). They have no sequence homology with either PcTx1 or APETx2, two toxins that we previously identified to target ASIC channels[13, 14]. A 3D-model of mambalgin-1 has been established from a pool of five templates with known structures (**Supplementary Fig. 1e**), which shows a

triple-stranded and a short double-stranded antiparallel β-sheets connecting loops II and III, and loop I, respectively, the three loops emerging from the core of the toxin like fingers from a palm (**Fig. 1b**). The model structure presents a concave face commonly found in neurotoxins and is stabilized by four disulfide bonds with a pattern identical to that observed in the crystal structure template (Cys1-Cys3, Cys2-Cys4, Cys5-Cys6 and Cys7-Cys8; **Fig. 1b** and **Supplementary Fig. 1f**). Mambalgins show a strong positive electrostatic potential that may contribute to binding to negatively charged ASIC channels (**Fig. 1c**).

Mambalgins have the unique property to be potent, rapid and reversible inhibitors of recombinant homomeric ASIC1a and heteromeric ASIC1a+ASIC2a or ASIC1a+ASIC2b channels, *i.e.*, all the ASIC channel subtypes expressed in the central nervous system[15-18], with a similar potency for both isopeptides and $IC_{50's}$ of 55 nM, 246 nM and 61 nM, respectively (**Fig. 1d**). Mambalgins also inhibit human ASIC channels (**Supplementary Fig. 2a**). The peptides inhibit ASIC1b and ASIC1a+ASIC1b channels that are specific of sensory neurons[19] with $IC_{50's}$ of 192 nM and 72 nM, respectively (**Fig. 1e**). Mambalgins, which bind to the closed and/or inactivated state of the channels (**Supplementary Fig. 2b**), modify the affinity for protons ($pH_{0.5act}$ shifted from 6.35 ± 0.04 to 5.58±0.02, and $pH_{0.5inact}$ shifted from 7.10±0.01 to 7.17±0.01, n=4, $p<0.001$ and n=5, $p<0.05$, respectively; **Fig. 1f**) and act as gating modifier toxins. They potently inhibit native ASIC currents in spinal cord, hippocampal and sensory neurons (**Fig. 1g,h** and **Supplementary Fig. 3**). In central spinal cord neurons, mambalgin-1 (674 nM) decreased ASIC current amplitude to 13.0 ± 2.0 % (n=14) of the control (**Fig. 1g**) and reduced the excitability in response to acidic pH without unspecific effect on basal neuronal excitability (resting potential), nor on the threshold and the shape of evoked or spontaneous action potentials and on spontaneous postsynaptic currents (**Supplementary Fig. 4**). Mambalgins had no effect on ASIC2a, ASIC3, ASIC1a+ASIC3 and ASIC1b+ASIC3 channels, as well as on TRPV1, P2X2, 5-HT_{3A}, Nav1.8, Cav3.2 and Kv1.2 channels (**Supplementary Figs. 5 and 6**).

Most three-finger toxins, like α-neurotoxins that block nicotinic acetylcholine receptors[20], evoke neurotoxic effects in animals. This is not the case of mambalgins, which do not produce motor dysfunction (**Supplementary Fig. 7**), apathy, flaccid paralysis, convulsions or death upon central injections (*i.t.* or *i.c.v.*) in mice, but instead induce analgesic effects against acute and inflammatory pain (**Fig. 2**) that can be as strong as morphine but resistant to naloxone, with much less tolerance (**Fig. 3a**) and no respiratory distress (**Fig. 3b**). In the tail-flick and paw-flick tests, *i.t.* injection of mambalgin-1 (or mambalgin-2) increased the latency for the tail and paw withdrawal reflex from 8.8 ± 0.4 s and 8.0 ± 0.8 s to 23.2 ± 1.3 s and 19.8 ± 1.6 s, respectively, seven minutes after injection (n=15-22, $p<0.001$) (**Fig. 2a,b**). The effects were completely lost in ASIC1a knockout mice (**Fig. 2a,b**), demonstrating the essential implication of ASIC1a-containing channels. The key involvement of ASIC channels present in central neurons in the analgesic effect of mambalgins was confirmed using *i.c.v.* injections of the peptides (**Supplementary Fig. 8**). Mambalgin-1 also suppressed inflammatory heat hyperalgesia and produced a strong analgesia evaluated in the paw-flick test after intraplantar (*i.pl.*) injection of carrageenan (**Fig. 2c**), and drastically decreased acute (phase I) and inflammatory (phase II) pain assessed in the formalin test (**Fig. 2d**), with a potency similar to morphine (**Fig. 2c,d)**. These effects were not significantly decreased by naloxone.

Mambalgins, unlike the spider peptide PcTx1[5, 14], inhibit not only homomeric ASIC1a channels, but also heteromeric ASIC1a+ASIC2 channels, which are abundantly expressed in central neurons[15-17, 21, 22]. This led us to analyse the participation of ASIC2 in central analgesia evoked by mambalgins. Intrathecal injections of siRNA to silence either ASIC2 (both variants

a and b) or ASIC2a (**Supplementary Fig. 9**) induced an analgesia that was partially (ASIC2) or fully (ASIC2a) resistant to naloxone (**Fig. 3c**). In the presence of naloxone, central injection of mambalgin-1 in these knockdown mice had a decreased effect (**Fig. 3d**), consistent with a contribution of ASIC2a in the pain suppressing effect of the peptide. Compensation by homomeric ASIC1a channels[15, 16], which are also blocked by mambalgin-1, as well as incomplete *in vivo* knockdown (**Supplementary Fig. 9**) account for the residual analgesic effect that is observed.

Because mambalgins are able to target different ASIC channel subtypes expressed in nociceptors, we have tested their peripheral effect after intraplantar injections. Mambalgin-1 (unlike PcTx1) has a significant analgesic effect on acute heat pain (**Fig. 4a**) and reverts or prevents inflammatory hyperalgesia (**Fig. 4b,c**). However, this effect is clearly different from the previously described effect of central (*i.t.*) injection of the peptide because it is still present in ASIC1a knockout mice (**Fig. 4a-c**) contrary to the central effect (**Fig. 2a,b**). If ASIC1a is not involved, what are then the mechanisms that support the peripheral effect of mambalgins? ASIC1b is specifically expressed in nociceptors[19, 23] but its role in pain is not known. A functional expression of ASIC1b-containing channels in DRG neurons is demonstrated by the effect of mambalgin-1, which blocks both ASIC1a and ASIC1b, and has more potent effects than PcTx1, which only blocks ASIC1a channels (**Fig. 1h**). Moreover, silencing of the ASIC1b subunit in nociceptors of ASIC1a knockout mice (*i.e.*, where only ASIC1b is present; **Supplementary Fig. 9**) mimicked the analgesic effect of peripheral injection of mambalgin-1 on both acute pain and inflammatory hyperalgesia, and largely decreased the effect of subsequent *i.pl.* injection of the peptide (**Fig. 4d,e**), supporting the specific participation of ASIC1b in the peripheral effect of mambalgin-1.

Our results indicate that mambalgins have analgesic effects by targeting both primary nociceptors and central neurons, but through different ASIC subtypes (**Supplementary Fig. 12**). After demonstrating the important role of ASIC3 in peripheral pain and sensory perception in the skin[3, 4, 24], we now show that ASIC1b, but not ASIC1a, is important for cutaneous nociception and inflammatory hyperalgesia. In the central nervous system, injections of mambalgins evoke a naloxone-insensitive analgesia through an opioid-independent pain pathway involving ASIC1a+ASIC2a channels. Central injections of PcTx1, instead, evoke a naloxone-sensitive analgesia through its specific action on homomeric ASIC1a [5,] and probably heteromeric ASIC1a+ASIC2b channels (**Fig. 3c** and [22]). In addition, mambalgins, unlike PcTx1[5], maintain a potent analgesia in mice deficient for the preproenkephalin gene (**Supplementary Fig. 10**). These results taken together indicate that different pathways involving different subtypes of ASIC channels can lead to different type of central analgesia (opioid-sensitive or insensitive) (**Supplementary Fig. 12**). They also indicate that in spite of their capacity *in vitro* to inhibit homomeric ASIC1a and heteromeric ASIC1a+ASIC2b channels, *in vivo*, mambalgin central analgesic action is mainly targeted to neurons expressing ASIC1a+ASIC2a channels (**Supplementary Fig. 11**).

It is essential to better understand pain in view to develop new analgesics[25, 26]. The black mamba peptides discovered here have the potential to address both of these aims. They reveal a potent role for different ASIC channel subtypes in both the central and peripheral pain pathways, providing novel promising targets for therapeutic interventions against pain, and they are themselves, at the same time, powerful naturally occurring analgesic peptides of potential therapeutic value.

References

1. Lewis, R.J. & Garcia, M.L. Therapeutic potential of venom peptides. *Nat Rev Drug Discov* **2**, 790-802 (2003).
2. Terlau, H. & Olivera, B.M. Conus venoms: a rich source of novel ion channel-targeted peptides. *Physiol Rev* **84**, 41-68 (2004).
3. Deval, E.*, et al.* Acid-sensing ion channels in postoperative pain. *J Neurosci* **31**, 6059-6066 (2011).
4. Deval, E.*, et al.* ASIC3, a sensor of acidic and primary inflammatory pain. *EMBO J* **27**, 3047-3055 (2008).
5. Mazzuca, M.*, et al.* A tarantula peptide against pain via ASIC1a channels and opioid mechanisms. *Nat Neurosci* **10**, 943-945 (2007).
6. Vanegas, H. & Schaible, H. Effects of antagonists to high-threshold calcium channels upon spinal mechanisms of pain, hyperalgesia and allodynia. *Pain* **85**, 9-18 (2000).
7. Schmidtko, A., Lotsch, J., Freynhagen, R. & Geisslinger, G. Ziconotide for treatment of severe chronic pain. *Lancet* **375**, 1569-1577 (2010).
8. Malmberg, A.B. & Yaksh, T.L. Effect of continuous intrathecal infusion of omega-conopeptides, N-type calcium-channel blockers, on behavior and antinociception in the formalin and hot-plate tests in rats. *Pain* **60**, 83-90 (1995).
9. Deval, E.*, et al.* Acid-sensing ion channels (ASICs): pharmacology and implication in pain. *Pharmacol Ther* **128**, 549-558 (2010).
10. Jones, N.G., Slater, R., Cadiou, H., McNaughton, P. & McMahon, S.B. Acid-induced pain and its modulation in humans. *J Neurosci* **24**, 10974-10979 (2004).
11. Bohlen, C.J.*, et al.* A heteromeric Texas coral snake toxin targets acid-sensing ion channels to produce pain. *Nature* **479**, 410-414 (2011).
12. Kini, R.M. & Doley, R. Structure, function and evolution of three-finger toxins: mini proteins with multiple targets. *Toxicon* **56**, 855-867 (2010).
13. Diochot, S.*, et al.* A new sea anemone peptide, APETx2, inhibits ASIC3, a major acid-sensitive channel in sensory neurons. *Embo J* **23**, 1516-1525 (2004).
14. Escoubas, P.*, et al.* Isolation of a tarantula toxin specific for a class of proton-gated Na+ channels. *J Biol Chem* **275**, 25116-25121 (2000).
15. Askwith, C.C., Wemmie, J.A., Price, M.P., Rokhlina, T. & Welsh, M.J. Acid-sensing ion channel 2 (ASIC2) modulates ASIC1 H+-activated currents in hippocampal neurons. *J Biol Chem* **279**, 18296-18305 (2004).
16. Baron, A., Voilley, N., Lazdunski, M. & Lingueglia, E. Acid sensing ion channels in dorsal spinal cord neurons. *J Neurosci* **28**, 1498-1508 (2008).
17. Lingueglia, E.*, et al.* A modulatory subunit of acid sensing ion channels in brain and dorsal root ganglion cells. *J Biol Chem* **272**, 29778-29783 (1997).
18. Waldmann, R., Champigny, G., Bassilana, F., Heurteaux, C. & Lazdunski, M. A proton-gated cation channel involved in acid-sensing. *Nature* **386**, 173-177 (1997).
19. Chen, C.C., England, S., Akopian, A.N. & Wood, J.N. A sensory neuron-specific, proton-gated ion channel. *Proc Natl Acad Sci U S A* **95**, 10240-10245 (1998).
20. Tsetlin, V. Snake venom alpha-neurotoxins and other 'three-finger' proteins. *Eur J Biochem* **264**, 281-286 (1999).
21. Baron, A., Waldmann, R. & Lazdunski, M. ASIC-like, proton-activated currents in rat hippocampal neurons. *J Physiol* **539**, 485-494 (2002).
22. Sherwood, T.W., Lee, K.G., Gormley, M.G. & Askwith, C.C. Heteromeric Acid-Sensing Ion Channels (ASICs) Composed of ASIC2b and ASIC1a Display Novel Channel Properties and Contribute to Acidosis-Induced Neuronal Death. *J Neurosci* **31**, 9723-9734 (2011).

23. Bassler, E.L., Ngo-Anh, T.J., Geisler, H.S., Ruppersberg, J.P. & Grunder, S. Molecular and functional characterization of acid-sensing ion channel (ASIC) 1b. *J Biol Chem* **276**, 33782-33787. (2001).
24. Fromy, B., Lingueglia, E., Sigaudo-Roussel, D., Saumet, J.L. & Lazdunski, M. Asic3 is a neuronal mechanosensor for pressure-induced vasodilation that protects against pressure ulcers. *Nat Med* doi:10.1038/nm.2844 (2012).
25. Basbaum, A.I., Bautista, D.M., Scherrer, G. & Julius, D. Cellular and molecular mechanisms of pain. *Cell* **139**, 267-284 (2009).
26. Woolf, C.J. Overcoming obstacles to developing new analgesics. *Nat Med* **16**, 1241-1247 (2010).
27. Wemmie, J.A.*, et al.* The acid-activated ion channel ASIC contributes to synaptic plasticity, learning, and memory. *Neuron* **34**, 463-477 (2002).
28. Konig, M.*, et al.* Pain responses, anxiety and aggression in mice deficient in pre-proenkephalin. *Nature* **383**, 535-538 (1996).
29. Jasti, J., Furukawa, H., Gonzales, E.B. & Gouaux, E. Structure of acid-sensing ion channel 1 at 1.9 A resolution and low pH. *Nature* **449**, 316-323 (2007).

Acknowlegments
We are very grateful to M.P. Price and M.J. Welsh for their generous gift of the *ASIC1a*$^{-/-}$ mice, to A. Zimmer for kindly providing the *Penk1*$^{-/-}$ mice, to H. Schweitz and L. Beress for their gift of pre-purified peptidic fractions of black mamba venom, to J. Noël for cultures of hippocampal neurons and comments, to E. Deval, P. Inquimbert, A. Delaunay and M. Christin for discussions, to C. Heurteaux and N. Blondeau for help with stereotaxic injections, to A. Lazzari for support with plethysmography, to V. Thieffin, N. Leroudier, S. Boulakirba, T. Lemaire, C. Karoutchi, G. Marrane for technical assistance, and to C. Chevance for secretarial assistance. We thank E. Bourinet, F. Rassendren and M.B. Emerit for providing the Cav3.2, P2X2 and 5-HT3A cDNAs, respectively.
This work was supported by the Fondation pour la Recherche Medicale (FRM), the Association Française contre les Myopathies (AFM), and the Agence Nationale de la Recherche (ANR). Part of this work has been supported by EMMAservice under the EU contract Grant Agreement Number 227490 of the EC FP7 Capacities Specific Programme.

Author Contributions
S.D. and A.B. conducted a large part of the experiments including the screening and HPLC purification of mambalgins (S.D.) and pain experiments, analyzed the data and participated to the preparation of the manuscript. M.S. conducted the cloning of mambalgin cDNA and electrophysiological experiments. D. Douguet realized the 3-D modelling. S.S., A.S.D. and D. Debayle performed the MS experiments and the amino-acid sequencing. V.F. performed validation of the siRNAs and provided technical support. A. A. was associated with pain behavior experiments. M.L. contributed to initial aspects of the work and participated to the final preparation of the manuscript. E.L. supervised the project and participated to data analysis and manuscript preparation.

Author Information
Mambalgin-1 cDNA and mambalgin-1 and -2 protein sequences have been deposited in GenBank and UniProt Knowledgebase under accession numbers JX428743, B3EWQ5 and B3EWQ4, respectively.

M. Lazdunski is a founder of Theralpha and the president of its scientific advisory board. The company has taken an option on the mambalgin patent. The other authors declare no competing financial interests.

Correspondence and requests for materials should be addressed to A.B. (baron@ipmc.cnrs.fr) or E.L. (lingueglia@ipmc.cnrs.fr).

METHODS SUMMARY

Mambalgins were purified from *Dendroaspis polylepis polylepis* venom (Latoxan, France) using cation exchange and reverse phase chromatography steps. The molecular mass and peptide sequence were determined by Edman degradatation and/or MS/MS sequencing, and used to design primers for cloning the full-length mambalgin-1 cDNA from venom. The 3D-structure was modeled from five templates of three-finger snake toxins. Recordings of recombinant ASIC currents were done after expression in *Xenopus laevis* oocytes[14] and COS-7 cells, and patch-clamp recordings of native ASIC currents were obtained from primary cultures of mouse dorsal spinal cord neurons[16], hippocampal neurons and rat DRG neurons. Pain behavior experiments were performed in C57BL/6J mice after *i.t.* (or *i.c.v.*) injection of mambalgins (10 µl at 34 µM), PcTx1 (10 µl at 10 µM) or morphine (Cooper, 10 µl at 3.1 mM), in the absence or in the presence of naloxone (Fluka, 2mg kg^{-1}), and after *i.pl.* injection of mambalgins (10 µl at 34 µM) and PcTx1 (10 µl at 10 µM). The effects of mambalgins on acute pain were also tested in *ASIC1a*$^{-/-}$[27] and *Penk1*$^{-/-}$[28] mice. Inflammation was evoked by *i.pl.* 2% carrageenan (Sigma) or 2% formalin. *In vivo* ASIC1 and ASIC2 gene silencing experiments were carried out by repeated *i.t.* injections (2 µg per mouse twice a day for 3 days) of siRNAs targeting ASIC1a+b, ASIC2a+b, or only ASIC2a, mixed with i-Fect (Neuromics) as previously described[4].

Figure 1. Mambalgins represent a new class of three-finger toxins targeting ASIC channels.

a, Black mamba venom (0.1 mg ml^{-1}) reversibly inhibits rat ASIC1a current expressed in *Xenopus* oocytes. **b**, 3D-model of mambalgin-1 (disulfide bridges in yellow). **c**, Electrostatic properties of mambalgin-1 and human ASIC1a channel (based on the 3D structure of chicken ASIC1a[29]) with positive and negative isosurfaces in blue and red, respectively. **d,e**, Inhibition of rat ASIC channels expressed in COS-7 cells (n=4-15; peptides applied before the pH drop as in **a**). Hill coefficients of 0.7-1 suggest a 1:1 stoichiometry between mambalgins and channels. **f**, Effect of mambalgin-1 on the pH-dependent activation and inactivation of ASIC1a current recorded in *Xenopus* oocytes (protocol shown in inset). **g,h**, Inhibition of native ASIC currents in dorsal spinal cord neurons (**g**) and DRG neurons (**h**) by mambalgin-1 (Mamb-1; 674 nM) and PcTx1 (20 nM), n=14-34. Right panels: effect of mambalgin-1 on neurons expressing no PcTx1-sensitive current. (Vh=-60 mV in **a**,**d**,**e** and -50mV in **f**,**g**,**h**). Mean ±SEM.

Figure 2. Intrathecal injections of mambalgin-1 exert potent naloxone-resistant and ASIC1a-dependent analgesia in mice.

a, b, Effects on acute thermal pain (46°C) determined using tail-immersion (**a**, n=13-22) and paw-immersion (**b**, n=5-15) tests showing a large increase in response latencies, which is lost in *ASIC1a*$^{-/-}$ mice; **c**, Effects on inflammatory hyperalgesia induced by *i.pl.* carrageenan (n=8-16). Right panels in **a-c;** Area Under Curve (AUC) calculated from each mouse. **d**, Effects on first (0-10 min) and second (10-45 min) phase of formalin-induced spontaneous pain behavior (n=11-20). Naloxone (Nalox) was injected *s.c.* 10 minutes before the peptide. Mamb-1, mambalgin-1; CAR, carrageenan; Veh, vehicle; comparison *vs* vehicle unless specified. Mean ± SEM.

Figure 3. The central analgesic effect of mambalgin-1 shows reduced tolerance as compared to morphine, no respiratory depression, and involves the ASIC2a subunit.

a, Repeated *i.t.* injections of mambalgin-1 induce less tolerance than morphine at concentrations giving the same analgesic efficacy (n= 10, comparison with vehicle * or morphine #). **b**, Mambalgin-1 (*i.t.*) induces no respiratory depression contrary to morphine (*i.t.* or *i.p.*, 0.01 and 0.4 mg per mice, respectively; n=4-7, comparison with vehicle unless specified). **c,** Paw-flick latency before (control) and after treatment with non-specific siRNA (si-CTR, n=24), siRNA against ASIC2a and ASIC2b (si-ASIC2a/2b, n=27), or siRNA against ASIC2a (si-ASIC2a, n=19) with or without naloxone. Comparison with si-CTR (#) or untreated control (*), unless specified. **d,** Paw-flick AUC calculated after *i.t.* injection of mambalgin-1 or vehicle in siRNA-treated mice (n=5-27; protocol shown in inset). Comparison with mice injected with vehicle after treatment by si-CTR, unless specified. Mean ± SEM.

Figure 4. Intraplantar injections of mambalgin-1 evoke peripheral analgesic effects *via* ASIC1b-containing channels.

a, Effects of mambalgin-1 on acute thermal pain (46°C) in wild-type (WT) and *ASIC1a*$^{-/-}$ mice (n=10-23). **b**, Effects of mambalgin-1 on carrageenan-induced hyperalgesia when injected before (open symbols) or 2h after (closed symbols) carrageenan (n=7-20). Right panels, AUC (after CAR in **b**). Comparison with vehicle unless specified. **c**, Mambalgin-1 prevents inflammatory hyperalgesia when co-injected with carrageenan (n=7-20, comparison with control). **d**, Paw-flick latency before (control) and after treatment with si-CTR (n=13) or siRNA against ASIC1a and ASIC1b (si-ASIC1a/1b, n=10) in *ASIC1a*$^{-/-}$ mice upon normal and inflammatory conditions. Comparison with si-CTR (#) or untreated control (*), unless specified. **e,** Paw-flick AUC calculated after injection of mambalgin-1 or vehicle in siRNA-treated *ASIC1a*$^{-/-}$ mice (n=7-11). Comparison with mice injected with vehicle after treatment by si-CTR, unless specified. Mean ± SEM.

METHODS

Electrophysiology in *Xenopus laevis* oocytes

Venom fractions were tested on rat ASIC1a expressed in *Xenopus* oocytes as previously described[14], applied 30 s before the acid stimulation.

Purification, peptide sequencing and mass spectrometry

The venom of the black mamba *Dendroaspis polylepis polylepis* (Latoxan, France) was purified by gel filtration and cation exchange[30]. The active fraction was loaded on a reversed-phase column (C18 ODS, Beckman) and eluted with a linear gradient of acetonitrile containing 0.1% TFA. Molecular mass and peptide sequence were determined by MALDI-TOF/TOF-MS (Applied Biosystems, USA). Protein identification was performed with mascot (http://www.matrixscience.com) at 50 ppm mass tolerance against NCBI (non redundant) and Swiss-Prot databases. Data were analyzed using the GRAMS386 software. Partial sequence was obtained by N-terminal Edman degradation and protease digestion (V8 protease and trypsin) followed by MS/MS sequencing. Peptide analysis was carried out using a nano-HPLC offline (DIONEX, U3000) coupled with a 4800 MALDI-TOF/TOF mass spectrometer.

Cloning of the mambalgin-1 cDNA

Mambalgin-1 cDNA was cloned from the black mamba venom[31]. Lyophilized venom (Sigma) was reconstituted in lysis/binding buffer and polyadenylated mRNAs were captured on oligo(dT25) magnetic beads (Dynal, UK). After first strand cDNA synthesis, PCR-amplification was done with degenerated sense (TGITTYCARCAYGGIAARGT) and antisense (YTTIARRTTICGRAAIGGCAT) primers designed from the partial peptide sequence obtained from biochemical purification. A specific sense primer (ACACGAATTCGCTATCATAACACTGGCATG) was designed from the new sequence and used with an unspecific poly-dT30 antisense primer (ACACGAATTCdT30) to amplify the 3'-coding and uncoding sequences of mambalgin-1. Using the very strong conservation of the 3'- and 5'-uncoding sequences among snake toxins[32], we have designed a sense (ACACGAATTCTCCAGAGAAGATCGCAAG***ATG***) and an antisense (ACACGAATTC-ATTTAGCCACTCGTAGAG***CTA***) primer to amplify the complete open reading frame of the toxin precursor.

Template-based 3D-Modeling of mambalgin-1

We modeled the mambalgin-1 protein using the semi-automatic pipeline of the webserver @TOME v2.1[33]. The amino acid sequence was submitted to the server to perform the fold recognition and detect structural homolog templates from the Protein Data Bank (PDB). Active fold-recognition tools were HHSEARCH[34], SP3[35], PsiBlast[36] and Fugue[37]. Five templates were selected among snake venom toxins with four disulfide bonds and aligned with Muscle[38]. The homology modeling of mambalgin-1 was performed with Modeller9v8. The overall quality of models was estimated by calculating the 1D/3D compatibility TITO score[39], by analyzing the ramachandran by Molprobity and comparing it to scores of the templates[40] and by visual inspection.

Electrostatic potential calculation

Electrostatic properties of mambalgin-1 (isosurfaces of +3 kbT/ec (~ + 77 mV) and -3 KbT/ec (~ -77 mV)) and human ASIC1a channel (isosurfaces of +10 kbT/ec (~ +256 mV) and -10 KbT/ec (~ -256 mV)) have been calculated with the Poisson-Boltzmann Solver APBS[41].

Electrophysiology in COS cells and neurons.

COS-7 cells were transfected with **pCI-ASICs** mixed with **pIRES2-EGFP** and jet-PEI. Primary cultures of dorsal spinal neurons were obtained from C57Bl6J mice embryos (E14)[16]. Primary cultured hippocampal neurons were prepared from C57Bl6J mice (P3-P5) as previously described for rats[42]. Primary cultured sensory neurons were prepared from dorsal root ganglia of Wistar rats (5-7 weeks) as previously described[43].

Data were recorded in the whole-cell configuration, sampled at 3.3 kHz and low-pass filtered at 3 kHz using pClamp8 software (Axon Instruments). Pipette solution (in mM): KCl 140, NaCl 5, $MgCl_2$ 2, EGTA 5, HEPES-KOH 10 (pH 7.4), bath solution (in mM): NaCl 140, KCl 5, $MgCl_2$ 2, $CaCl_2$ 2, HEPES-NaOH 10 (pH 7.4). MES was used instead of HEPES for pH from 6 to 5. The bath solution for neurons was supplemented with 10 mM glucose, and 20 µM CNQX/ 10 µM kynurenic acid for central neurons. The pipette solution for neurons contained (in mM): KCl 140, ATP-Na_2 2.5, $MgCl_2$ 2, $CaCl_2$ 2, EGTA 5, HEPES 10 (pH 7.3, pCa estimated to 7). Toxins were perfused at pH 7.4 with bovine serum albumin (0.05%) to prevent non-specific adsorption. Concentration-response curves were fitted by the Hill equation: $I = Imax + (Imin-Imax) (C^{nH}/(C^{nH}+ IC_{50}^{nH}))$ where I is the amplitude of relative current, C is the toxin concentration, IC_{50} is the toxin concentration half-maximally inhibited the current, and n_H is the Hill coefficient.

Plethysmography

Respiratory frequency (breaths min^{-1}) was recorded from 7 min to 67 min after *i.t.* injection of vehicle, mambalgin-1 or morphine-HCl (according the same protocol than for pain behavior) or *i.p.* injection of morphine-HCl (24.8 mM, 50 µl) with a whole-body plethysmograph (Emka Technologies).

Pain behavior experiments

Experiments were performed on awake 7-11 week-old (20-25g) male C57BL/6J, *ASIC1a*$^{-/-}$[27] and *Penk1*$^{-/-}$[28] mice following the guidelines of the International Association for the Study of Pain and were approved by the local ethic committee (Agreement NCA/2007/04-01 and NCE/2011-06). Mambalgin-1 (34 µM), mambalgin-2 (20 µM), PcTx1 (10µM) and morphine-HCl (3.1 mM; Cooper) dissolved in vehicle solution (in mM: NaCl 145, KCl 5, $MgCl_2$ 2, $CaCl_2$ 2, HEPES 10, pH 7.4, 0.05% BSA for *i.t.* injection, and NaCl 154, 0.05% BSA for *i.pl.* injection) were injected intrathecally (*i.t.,* 10 µl) between spinal L5 and L6 segments or intraplantarly (*i.pl.*, 10 µl). Naloxone (Fluka, 2 mg kg^{-1} in NaCl 0.9%, 50 µl) was subcutaneously (*s.c.*, dorsal injection) injected ten minutes before *i.t* injection. Inflammation was evoked by *i.pl.* injection in the left hindpaw of 2% carrageenan (Sigma-Aldrich) (20 µl) two hours before *i.t* or *i.pl*. injection of peptides, morphine or vehicle.

Knockdown experiments

Locally designed siRNAs targeting ASIC1 (si-ASIC1a/1b), GCCAAGAAGUUCAACAAAUdtdt), ASIC2 (si-ASIC2a/2b), UGAUCAAAGAGAAGCUAUUdtdt) and ASIC2a (si-ASIC2a, AGGCCAACUUCAAACACUAdtdt) have been validated *in vitro* in COS-7 cells transfected with myc-ASIC1a, ASIC1b, myc-ASIC2a or myc-ASIC2b, and the relevant siRNA or a control siRNA (si-CTR; GCUCACACUACGCAGAGAUdtdt) with TransIT-LT1 and transIT-TKO (Mirus, USA), respectively. Cells were lysed 48 h after transfection and processed for Western blot analysis to assess the level of ASIC1a protein with the anti-Myc A14 antibody (1:500; Santa Cruz Biotechnology) or the anti-ASIC1 antibody (N271/44; 1:300; NeuroMab) and a monoclonal antibody against actin (AC-40; 1:1,000; Sigma) as a loading control. siRNAs were *i.t.* injected in mice (2 µg/mouse at a ratio of 1:4 (w/v) with i-Fect (Neuromics)) twice a day for 3 days. After 3 days of treatment, the paw-flick latency was measured and the residual effect of mambalgin-1 (*i.t.* or *i.pl.*, 34 µM) or the CAR-induced hyperalgesia (*i.pl.*, 2%) was tested. For validation of the *in vivo* effect of the siRNAs, lumbar DRGs or lumbar dorsal spinal cord were removed after the last siRNA injection for total RNA isolation (RNeasy kits, Qiagen) followed by cDNA synthesis (AMV First-Strand cDNA synthesis kit, Invitrogen and High Capacity RNA-to-cDNA Kit, Applied Biosystems). The relative levels of ASIC transcripts were evaluated by quantitative reverse-transcription PCR in a Light-Cycler 480 (Roche Products). Pre-designed and validated TaqMan assays for ASIC1 (ASIC1a and ASIC1b; Mm01305998_mH), ASIC1a (Mm01305996_m1), ASIC2

(ASIC2a and ASIC2b; Mm00475691_m1), ASIC3 (Mm00805460_m1) and 18S ribosomal RNA (Mm03928990_g1) were from Applied Biosystems. Each cDNA sample was run in triplicate and results were normalized against 18S and converted to fold induction relative to control siRNA treatment.

Data analysis

Data analysis and statistics were performed with Microcal Origin 6.0 and GraphPad Prism 4 softwares. Areas under the time course curves (AUC, s.min) were calculated for each mouse (over the first 37 minutes for tail-flick and the entire time range for paw-flick) and expressed as mean ± SEM. After testing the normality of data distribution, the statistical difference between two different experimental groups was analyzed by unpaired Student's *t*-test, and between more than two different experimental groups by a two-way analysis of variance (Anova) followed by a Newman-Keuls multiple comparison test when $P<0.05$. For data within the same experimental group, a paired Student's *t*-test was used. *** or $^{###,}$ $p<0.001$; ** or $^{##}$, $p<0.01$; *, $p<0.05$, *ns*, $p>0.05$.

Supplementary references

30. Schweitz, H., Bidard, J.N. & Lazdunski, M. Purification and pharmacological characterization of peptide toxins from the black mamba (Dendroaspis polylepis) venom. *Toxicon* **28**, 847-856 (1990).
31. Chen, T.*, et al.* Unmasking venom gland transcriptomes in reptile venoms. *Anal Biochem* **311**, 152-156 (2002).
32. Nakashima, K.*, et al.* Accelerated evolution in the protein-coding regions is universal in crotalinae snake venom gland phospholipase A2 isozyme genes. *Proc Natl Acad Sci U S A* **92**, 5605-5609 (1995).
33. Douguet, D. & Labesse, G. Easier threading through web-based comparisons and cross-validations. *Bioinformatics* **17**, 752-753 (2001).
34. Soding, J. Protein homology detection by HMM-HMM comparison. *Bioinformatics* **21**, 951-960 (2005).
35. Zhou, H. & Zhou, Y. SPARKS 2 and SP3 servers in CASP6. *Proteins* **61 Suppl 7**, 152-156 (2005).
36. Altschul, S.F.*, et al.* Gapped BLAST and PSI-BLAST: a new generation of protein database search programs. *Nucleic Acids Res* **25**, 3389-3402 (1997).
37. Shi, J., Blundell, T.L. & Mizuguchi, K. FUGUE: sequence-structure homology recognition using environment-specific substitution tables and structure-dependent gap penalties. *J Mol Biol* **310**, 243-257 (2001).
38. Edgar, R.C. MUSCLE: multiple sequence alignment with high accuracy and high throughput. *Nucleic Acids Res* **32**, 1792-1797 (2004).
39. Labesse, G. & Mornon, J. Incremental threading optimization (TITO) to help alignment and modelling of remote homologues. *Bioinformatics* **14**, 206-211 (1998).
40. Chen, V.B.*, et al.* MolProbity: all-atom structure validation for macromolecular crystallography. *Acta Crystallogr D Biol Crystallogr* **66**, 12-21 (2010).
41. Baker, N.A., Sept, D., Joseph, S., Holst, M.J. & McCammon, J.A. Electrostatics of nanosystems: application to microtubules and the ribosome. *Proc Natl Acad Sci U S A* **98**, 10037-10041 (2001).
42. Fitzjohn, S.M.*, et al.* An electrophysiological characterisation of long-term potentiation in cultured dissociated hippocampal neurones. *Neuropharmacology* **41**, 693-699 (2001).
43. Mamet, J., Baron, A., Lazdunski, M. & Voilley, N. Proinflammatory mediators, stimulators of sensory neuron excitability via the expression of acid-sensing ion channels. *J Neurosci* **22**, 10662-10670 (2002).

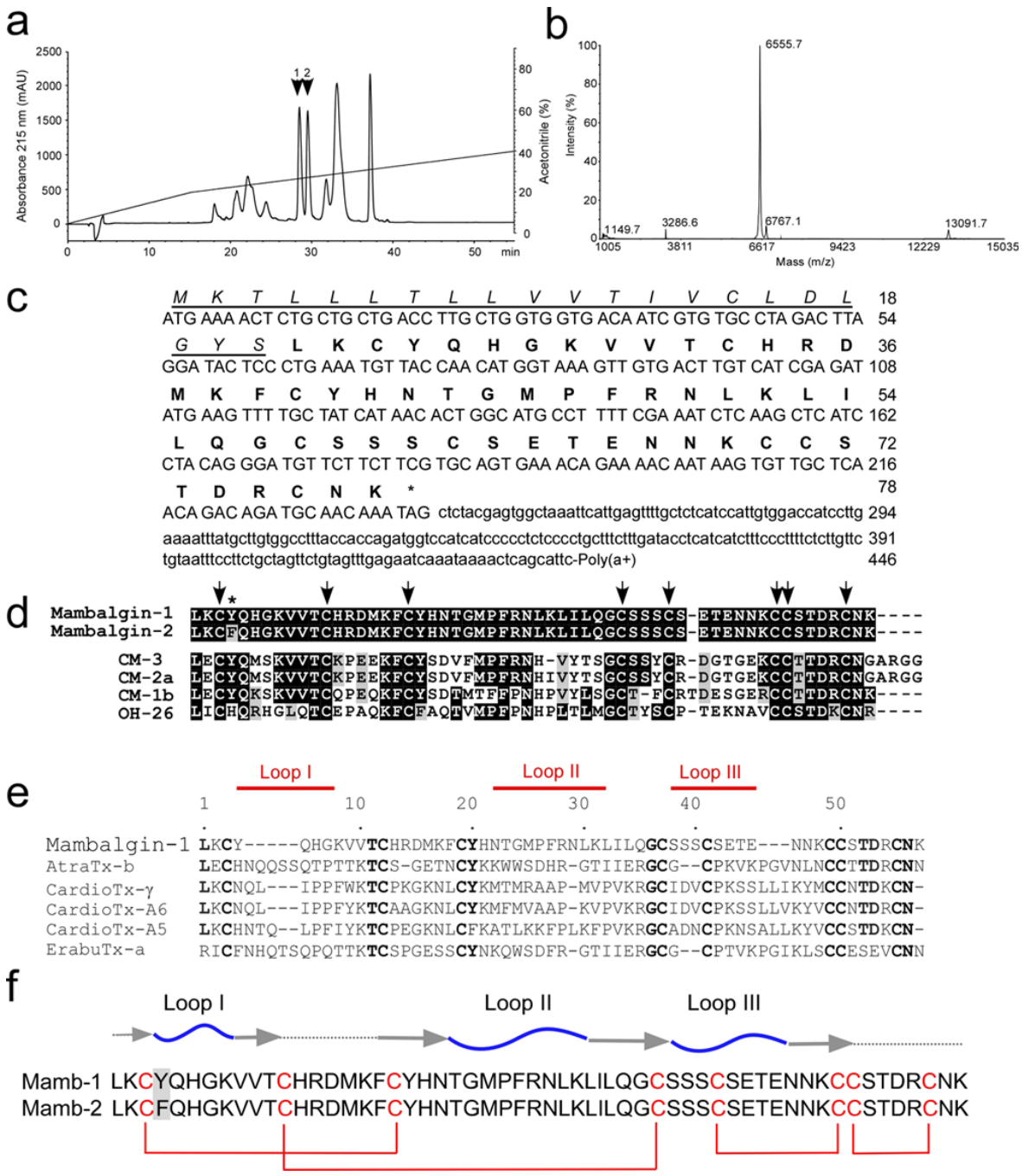

Supplementary Figure 1. Purification of mambalgins from *Dendroaspis polylepis polylepis* venom, cDNA, sequence comparisons with other toxins and secondary structure prediction.

a- Reverse phase HPLC profile of the peptide fraction active on ASIC1 currents. Peak 1 and 2 eluted at 26 and 27% of acetonitrile correspond to mambalgin-1 and mambalgin-2, respectively. The line indicates the gradient (% of acetonitrile) **b**- Mass spectrum of mambalgin-1 (peak 1, measured average molecular mass of 6554.7 Da). Measurement was performed using MALDI-TOF/TOF-MS. Mass spectrum was acquired in mass range of

1,000-16,000 Da using positive linear mode. **c**, Sequence of mambalgin-1 cDNA and the corresponding protein. Signal peptide (in italics and underlined) and final toxin (in bold) are displayed on top of the corresponding nucleotide sequence. **d**, Multiple protein sequence alignment of mambalgin-1 and mambalgin-2 (π-Dp1 and π-Dp2 according to the nomenclature proposed by King et al.[44]) with the most similar sequences from databases. CM-3 and CM-2a from *Naja haje annulifera* [45], CM-1b from *Hemachatus haemachatus* [46], the α-neurotoxin OH-26 from *Ophiophagus hannah* [47], all from cobra venoms, share 55%, 54%, 47% and 47% sequence identity with mambalgin-1, respectively (individual alignments with mambalgin-1, ClustalW). These peptides constitute a class of non-toxic peptides with no known target, which are immunochemically unrelated to the toxic "Naja type" cytotoxins and α-neurotoxins isolated from Elapid venoms. Amino acids that are identical or similar to mambalgin-1 are printed white on black or black on grey background, respectively. The eight highly conserved cysteine residues are shown with arrows. Position 4 that differs between mambalgin-1 and mambalgin-2 is marked by an asterisk. Note that the venom of *Naja haje annulifera*, which contains the CM-2a and CM-3 toxins, and the venom of *Ophiophagus hannah*, which contains the OH-26 toxin, have no significant effect on ASIC1a channels expressed in *Xenopus* oocytes (see Supplementary Fig. 5b**). e**, Mutiple sequence alignment with other snake three-finger toxins of known 3D structures that share the highest sequence identities with mambalgin-1 and have been chosen as templates for 3D-modeling of the toxin. The three loops are indicated on the top of the sequences by red lines. Residues in black are highly conserved between mambalgin-1 and the templates. Atratoxin-b from *Naja atra* (AtraTx-b, PDB 1VB0, [48]), Cardiotoxin-γ from *Naja nigricollis* (CardioTx-γ, PDB 1TGX, [49]), Cardiotoxin-A6 from *Naja atra* (CardioTx-A6, PDB 1UG4, [50]), Cardiotoxin-A5 from *Naja atra* (CardioTx-A5, PDB 1CVO, [51]), and Erabutoxin-a from *Laticauda semifasciata* (ErabuTx-a, PDB 3ERA, [52]) show 31%, 28%, 28%, 29% and 25% sequence identity with mambalgin-1, respectively (multiple alignment, MUSCLE). Cardiotoxin-A5, Cardiotoxin-A6 and Cardiotoxin-γ are cytotoxins known to bind to and disrupt the organization, integrity, and function of the cell membrane, and Atratoxin-b and Erabutoxin-a are two short neurotoxins known to bind to acetylcholine receptors. **f**, Sequence alignment of mambalgin-1 (Mamb-1) and mambalgin-2 (Mamb-2) and secondary structure prediction showing the localization of loops, β-strands (gray arrows) and disulfide bridges between the eight highly conserved cysteine residues (in red). Position 4 differs between mambalgin-1 and mambalgin-2.

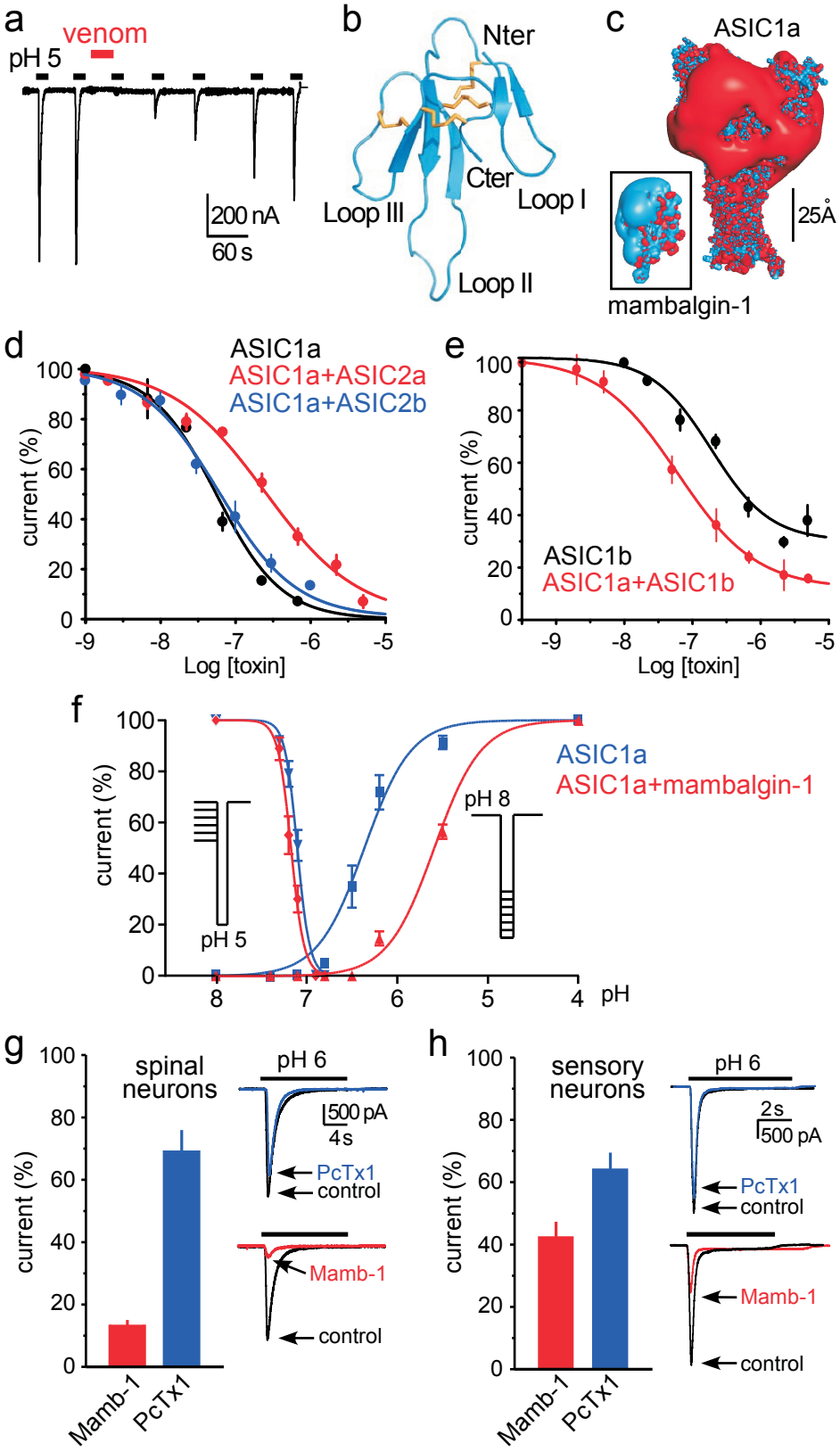
a
venom
pH 5
200 nA
60 s
b
Nter
Cter
Loop I
Loop III
Loop II
c
ASIC1a
25Å
mambalgin-1
d
ASIC1a
ASIC1a+ASIC2a
ASIC1a+ASIC2b
current (%)
Log [toxin]
e
ASIC1b
ASIC1a+ASIC1b
current (%)
Log [toxin]
f
ASIC1a
ASIC1a+mambalgin-1
pH 8
pH 5
current (%)
pH
g
spinal neurons
pH 6
500 pA
4 s
PcTx1
control
Mamb-1
control
current (%)
Mamb-1
PcTx1
h
sensory neurons
pH 6
2 s
500 pA
PcTx1
control
Mamb-1
control
current (%)
Mamb-1
PcTx1

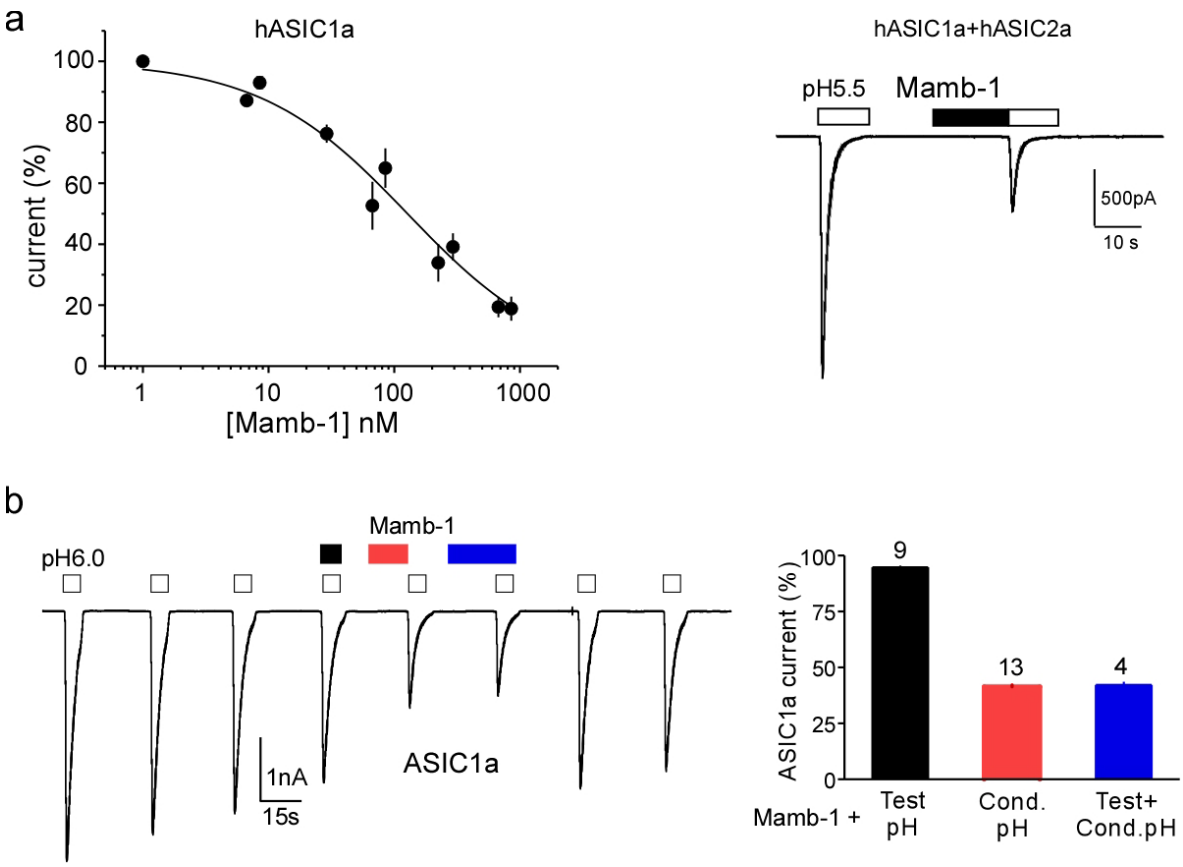

Supplementary Figure 2. Mambalgin-1 inhibits human ASIC1a and ASIC1a+ASIC2a channels and its effect on ASIC channels depends on the protocol for applying the toxin. **a**, Inhibition by mambalgin-1 (Mamb-1) of homomeric hASIC1a current (left panel, IC_{50}=127 nM, mean ± SEM, n=4-15) and heteromeric hASIC1a+hASIC2a current (right panel, Mamb-1 674 nM) expressed in COS-7 cells. ASIC currents were activated by rapid changes of the external pH from 7.4 to 5.5 (holding potential -60 mV). **b**, When mambalgin-1 (Mamb-1, 85nM) was applied only during the acid pH drop to 6.0 (Test pH) from pH 7.4, the toxin did not produce any blockade of rat ASIC1a current expressed in COS-7 cells (5.2±2.2%, n=9; Mean ± SEM, right panel). When mambalgin-1 was applied at pH 7.4 (conditioning pH, Cond. pH) 30s before the pH drop and kept during the stimulation (Test + Cond. pH), it produced an inhibition of the current similar to an application only at pH 7.4 (Cond. pH) (*i.e.*, without toxin during the pH drop) (58.6±3%, n=13 and 57.8±3%, n=4, respectively; Mean ± SEM, right panel). Holding potential -50 mV. Control and washout responses to pH before and after application of the peptide have been done for the distinct ways of applying the peptide. These data indicate that mambalgin-1 does not bind to the open channel but it is very difficult to distinguish between pH dependence for toxin binding to the channel from state-dependent binding *per se*.

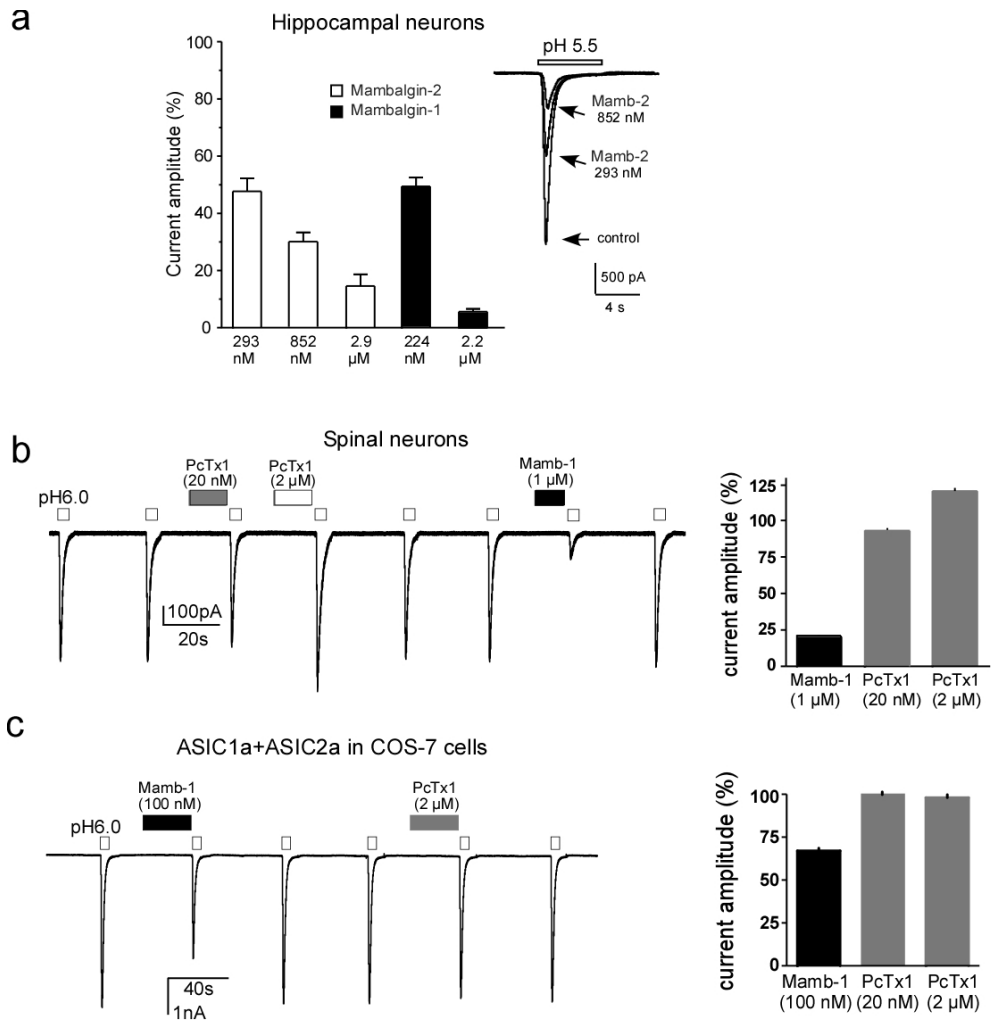

Supplementary Figure 3. Mambalgins inhibit native ASIC currents in hippocampal neurons, while a high concentration of PcTx1 does not inhibit native ASIC1a+ASIC2a like currents in spinal cord neurons or ASIC1a+ASIC2a channels expressed in COS cells.

a, Inhibition (% of control current) of ASIC current in mouse hippocampal neurons by mambalgin-1 (black bars) and mambalgin-2 (white bars). Mean ± SEM (n=26). Inset: currents recorded at -50 mV and activated by a drop in pH from 7.4 to 5.5. **b**, The native acid stimulated current evoked by a pH drop from 7.4 to 6.0 in the sub-population of spinal cord neurons expressing ASIC1a+ASIC2a channels (*i.e.*, neurons insensitive to PcTx1, 20 nM) is blocked by mambalgin-1 (Mamb-1, 1 µM) but not by PcTx1 at a similar concentration (2 µM, *i.e.*, ~100-fold the concentration used to block homomeric ASIC1a channels) (right panel, mean ± SEM, n=6-7). **c**, High concentration of PcTx1 (2 µM) is also without effect on ASIC1a+ASIC2a heteromeric channels expressed in COS-7 cells. Currents evoked by a pH drop from 7.4 to 6.0 (right panel, mean ± SEM, n=4-5). Holding potential -60 mV.

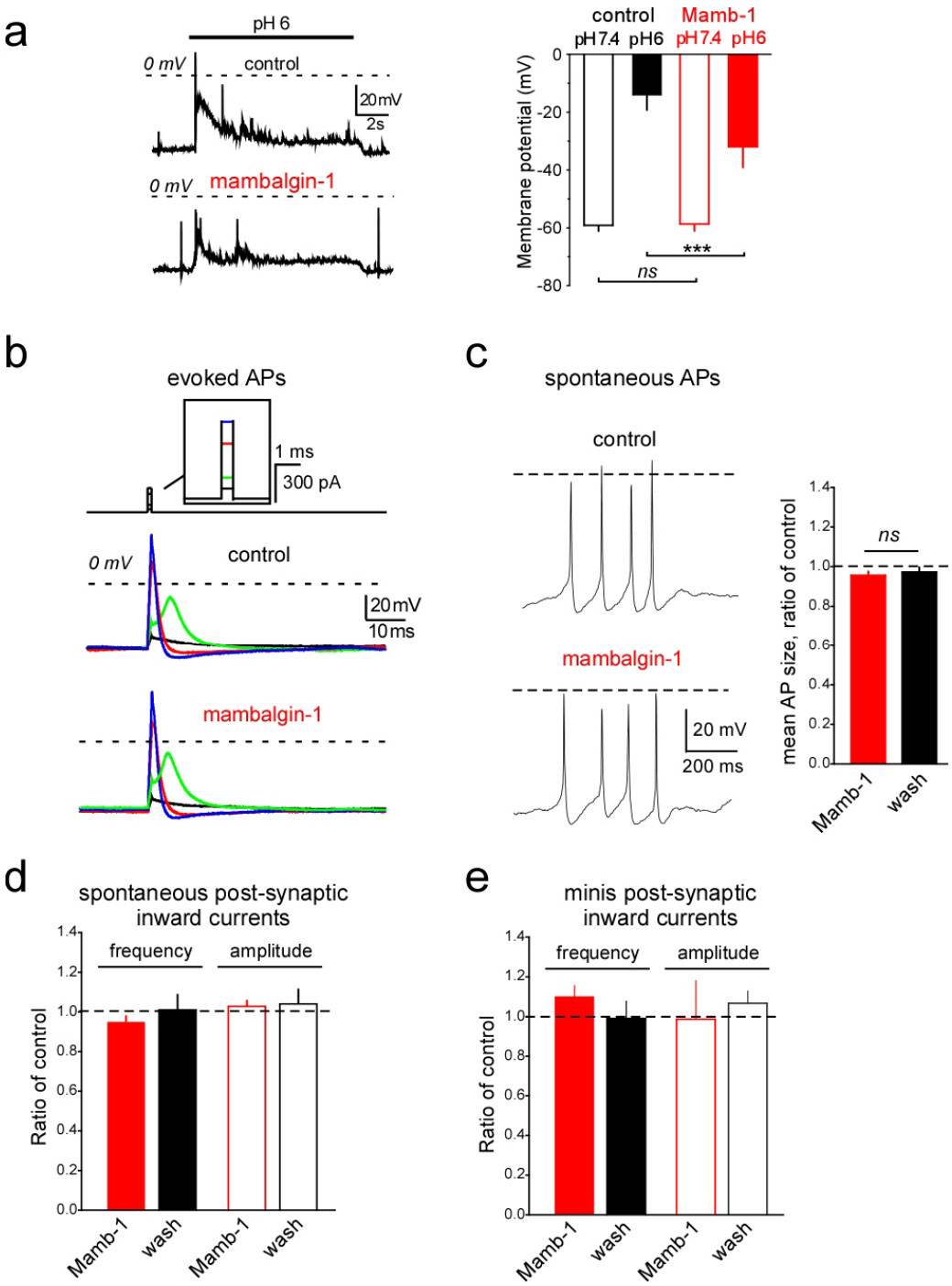

Supplementary Figure 4. Mambalgin-1 reduces the excitability in response to acidic pH without unspecific effect on basal neuronal excitability, on the threshold and the shape of evoked or spontaneous action potentials, and on spontaneous postsynaptic currents in primary cultured dorsal spinal neurons. a, Mambalgin-1 (674 nM) reduced the mean depolarisation (n=10) triggered by a pH drop from 7.4 to 6.0 without affecting the resting membrane potential in dorsal spinal cord neurons. Action potentials were excluded from membrane potential measurements. A typical recording is shown on the left. Mean ±SEM.

b, c Action potentials (APs) evoked by increasing current pulses (**b**) and spontaneous APs recorded in the absence of CNQX and kynurenic acid (**c**), showing no change in the shape and threshold of APs before and during local extracellular perfusion of mambalgin-1 (Mamb-1, 674 nM) at pH 7.4. Two membrane potential traces evoked by infraliminar current pulses and two evoked by supraliminar current pulses triggering action potentials are superimposed in **b**. Inset in **c** illustrates the lack of change in AP amplitude in the presence of Mamb-1 and after wash-out of the peptide (wash) expressed as a ratio of control. Mean ± SEM, n=3, paired *t*-test. **d**, No change in spontaneous post-synaptic inward currents amplitude and frequency in the presence of mambalgin-1 (674 nM) and after wash-out of the peptide (wash) expressed as a ratio of control. Holding potential -50 mV. Mean ± SEM, n=4, not significantly different by paired *t*-test. **e**, No change in miniature post-synaptic inward currents amplitude and frequency in similar conditions. Holding potential -50 mV. Mean ± SEM, n=3, not significantly different by paired *t*-test. Miniature currents were recorded in the presence of 0.3 µM tetrodotoxin (TTX). Analysis was performed with WinEDR and WinWCP programs of the Strathclyde Electrophysiology Software (courtesy of John Dempster, Strathclyde Institute of Pharmacy and Biomedical Sciences, University of Strathclyde, Glasgow, UK).

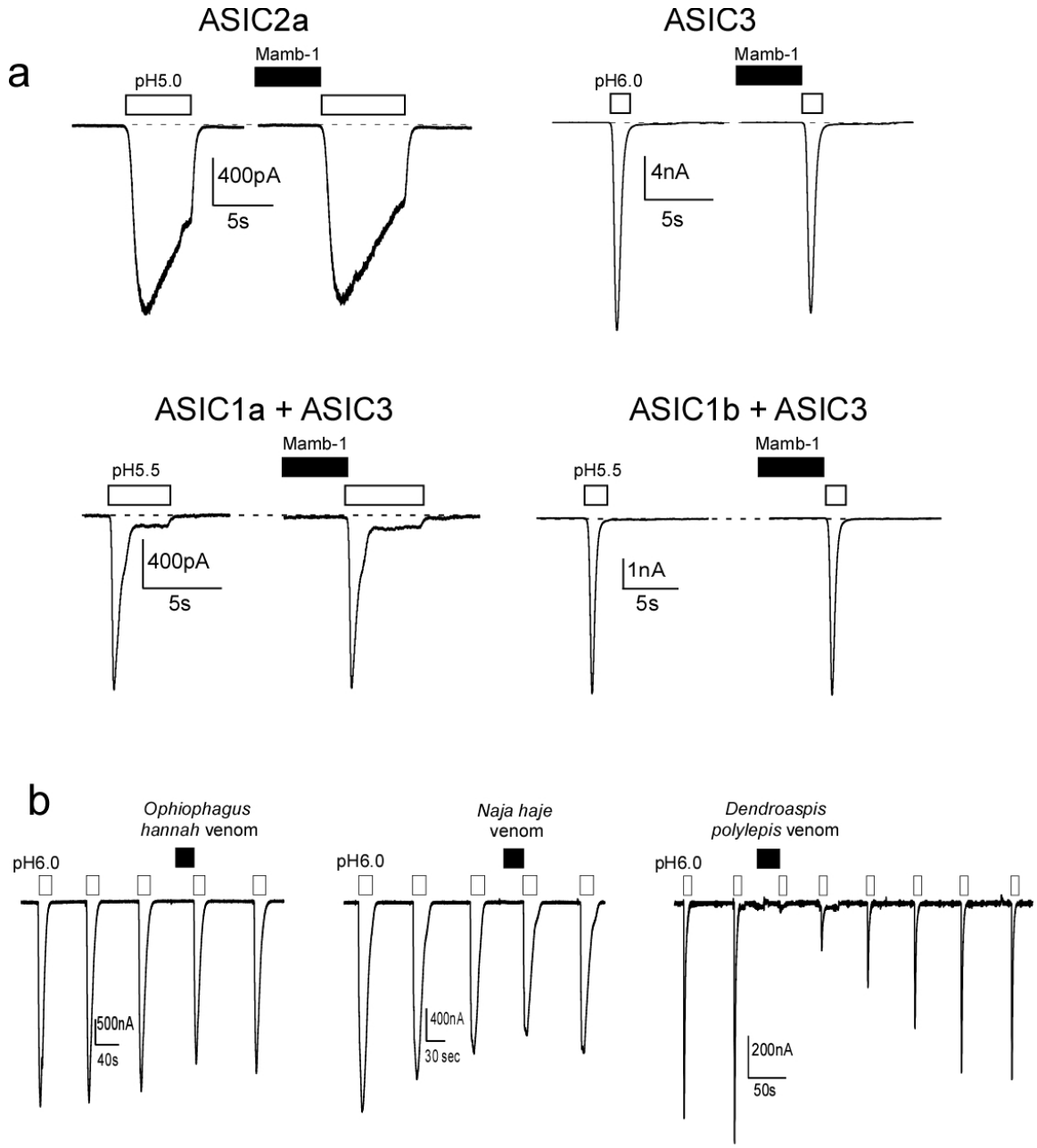

Supplementary Figure 5. Mambalgin-1 has no effect on ASIC2a, ASIC3, ASIC1a+ASIC3 and ASIC1b+ASIC3 channels, and venoms of *Naja haje annulifera* and *Ophiophagus hannah* do not inhibit ASIC1a channels.

a, Effect of mambalgin-1 (Mamb-1, 674nM) on homomeric and heteromeric ASIC channels expressed in COS-7 cells (4-13 cells tested). **b**, The venom of egyptian cobra *Naja haje annulifera* (0.01 mg ml^{-1}), which contains the CM-2a and CM-3 toxins, and the venom of king cobra *Ophiophagus hannah* (0.05 mg ml^{-1}), which contains the OH-26 toxin, have no significant effect on ASIC1a channels expressed in *Xenopus* oocytes contrary to the venom of black mamba *Dendroaspis polylepis* (0.01 mg ml^{-1}) (n=3-5). Each venom was perfused during 30-45s before the pH drop. Holding potential -60mV, conditioning pH 7.4.

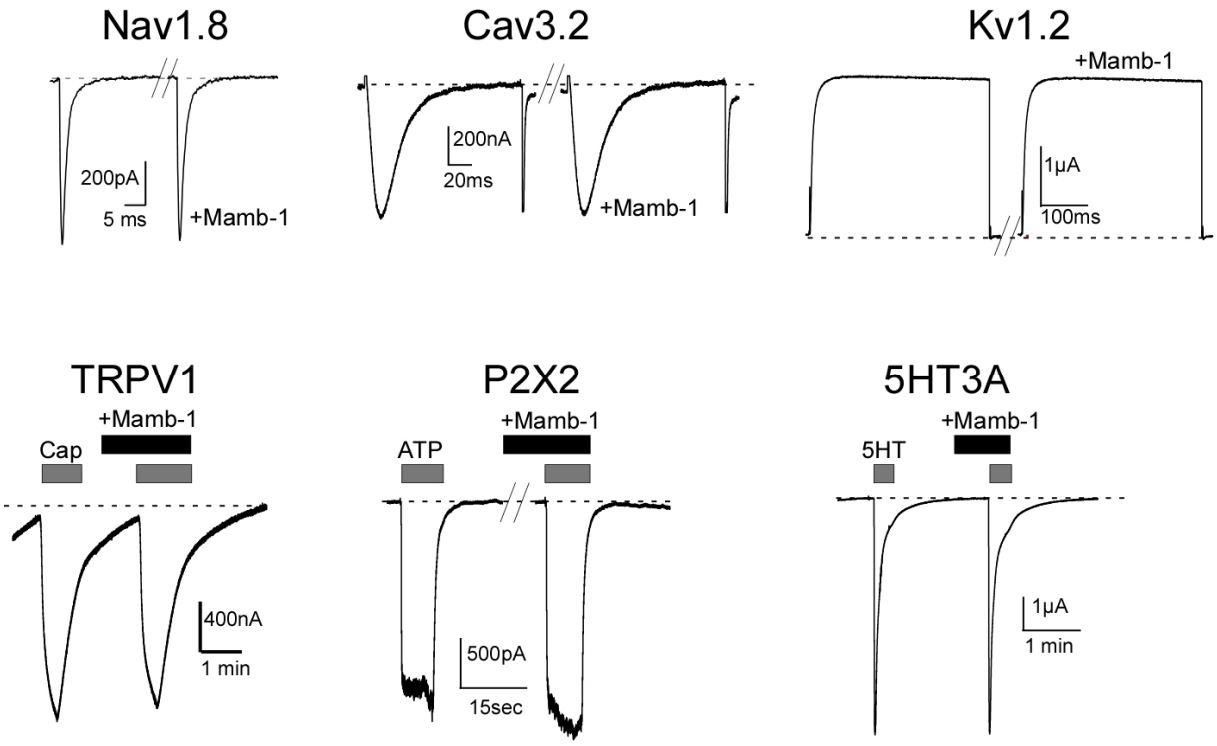

Supplementary Figure 6. Mambalgin-1 has no effect on a panel of different ligand-operated and voltage-activated channels.

Voltage-gated currents were recorded by depolarization every 10s to -20mV (hCav3.2 and Kv1.2 expressed in *Xenopus* oocytes) or to 0mV (Nav1.8 expressed in HEK 293 cells) from a holding potential of -80mV. Mambalgin-1 (Mamb-1, 3µM) was perfused continuously during depolarization steps and a representative trace is shown for each channel before and after 50-60s toxin application (n=4-5).

TRPV1, 5-HT3a (expressed in *Xenopus* oocytes) and P2X2 (expressed in COS-7 cells) were activated by their respective ligands (1µM capsaicin, 10µM ATP and 30µM 5-HT, respectively). Mambalgin-1 (3µM) was perfused continuously before (45s) and during the pH stimulation. No significant inhibition was observed (n=4-5).

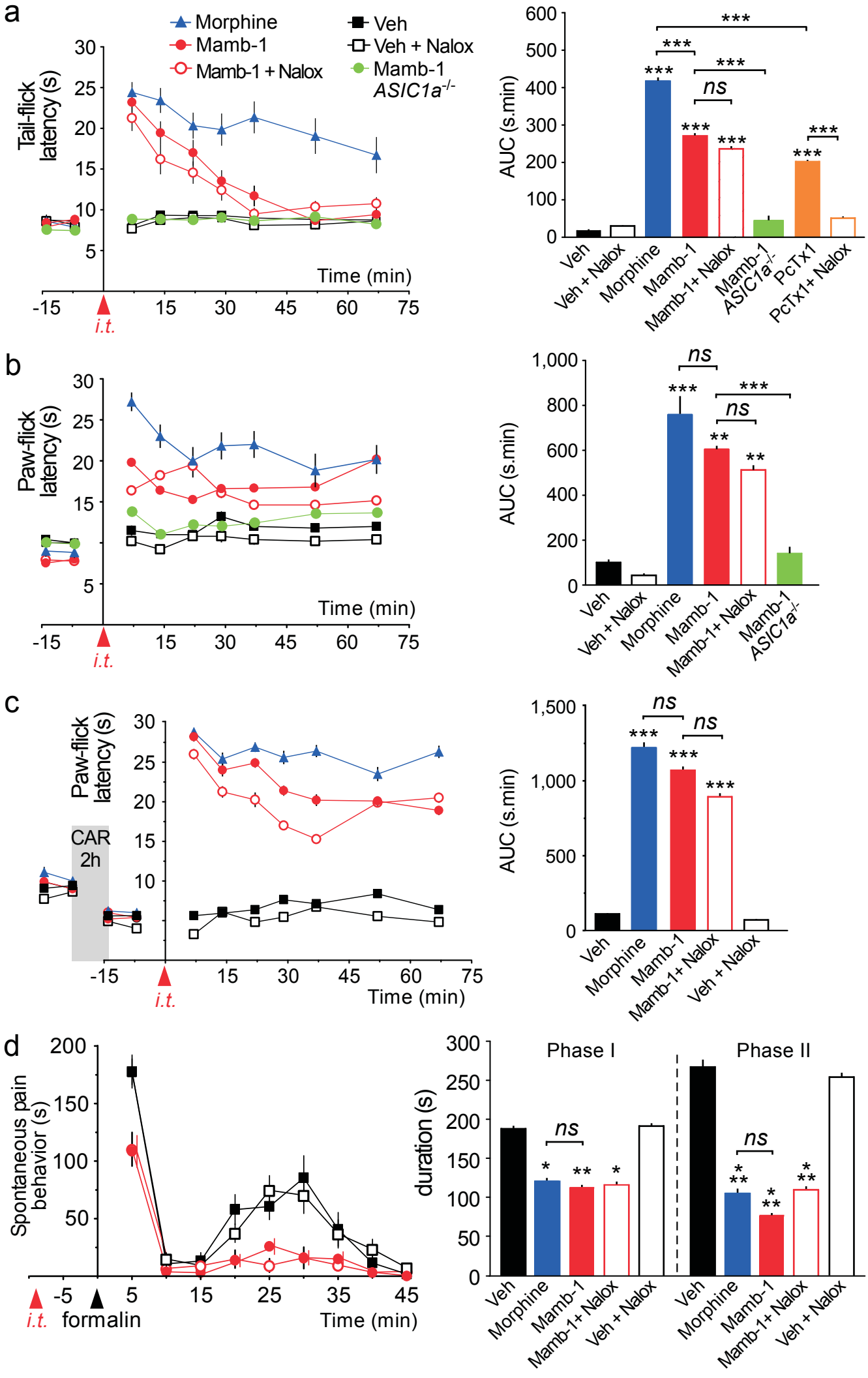
a
Morphine
Mamb-1
Mamb-1 + Nalox
Veh
Veh + Nalox
Mamb-1 ASIC1a-/-
Tail-flick latency (s)
Time (min)
i.t.
AUC (s.min)
Veh
Veh + Nalox
Morphine
Mamb-1
Mamb-1+ Nalox
Mamb-1 ASIC1a-/-
PcTx1
PcTx1+ Nalox
b
Paw-flick latency (s)
Time (min)
i.t.
AUC (s.min)
c
Paw-flick latency (s)
CAR 2h
i.t.
Time (min)
AUC (s.min)
d
Spontaneous pain behavior (s)
i.t.
formalin
Time (min)
duration (s)
Phase I
Phase II

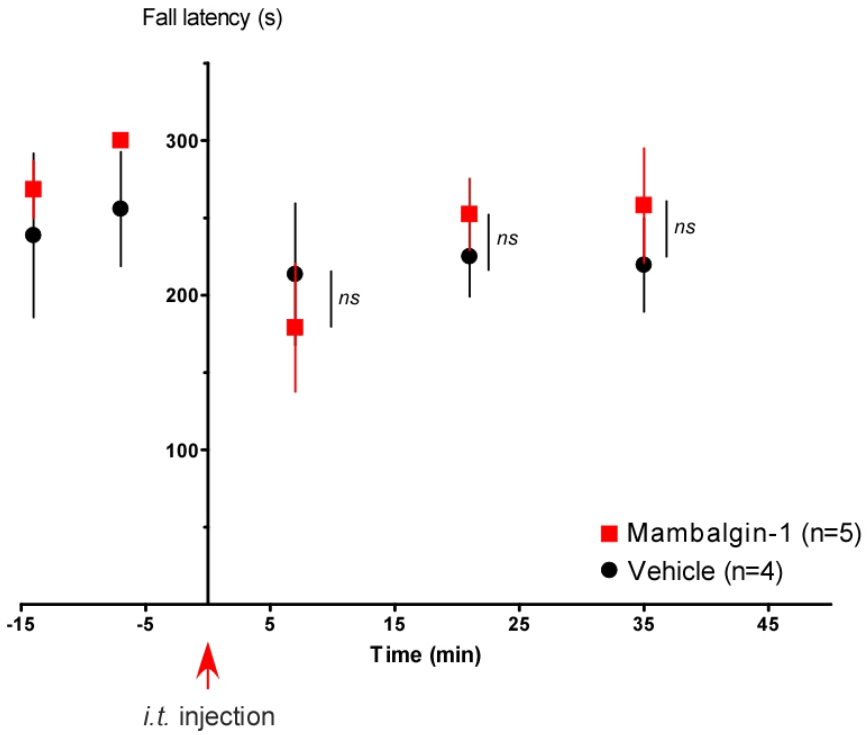

Supplementary Figure 7. Intrathecal injection of mambalgin-1 has no effect on mice motor behavior evaluated by the Rotarod test.

Time-course of fall latency (s) before and after an *i.t.* injection mambalgin-1 (34 µM, 10 µl) or vehicle. The mouse was placed onto the dowel with the accelerating Rota-rod treadmill (Ugo Basile) rotating at 4 rpm and then accelerating at a constant rate of 5 rpm min^{-1} up to 40 rpm [53]. The latency to fall to the floor was automatically recorded, with a maximum cut-off latency of 300 s. Two control trials were performed before *i.t.* injection, and test trials were then performed 7, 21 and 35 minutes after injection. Mean ± SEM. Intrathecal injection of mambalgin-1 induced no significant change in motor activity (unpaired *t*-test).

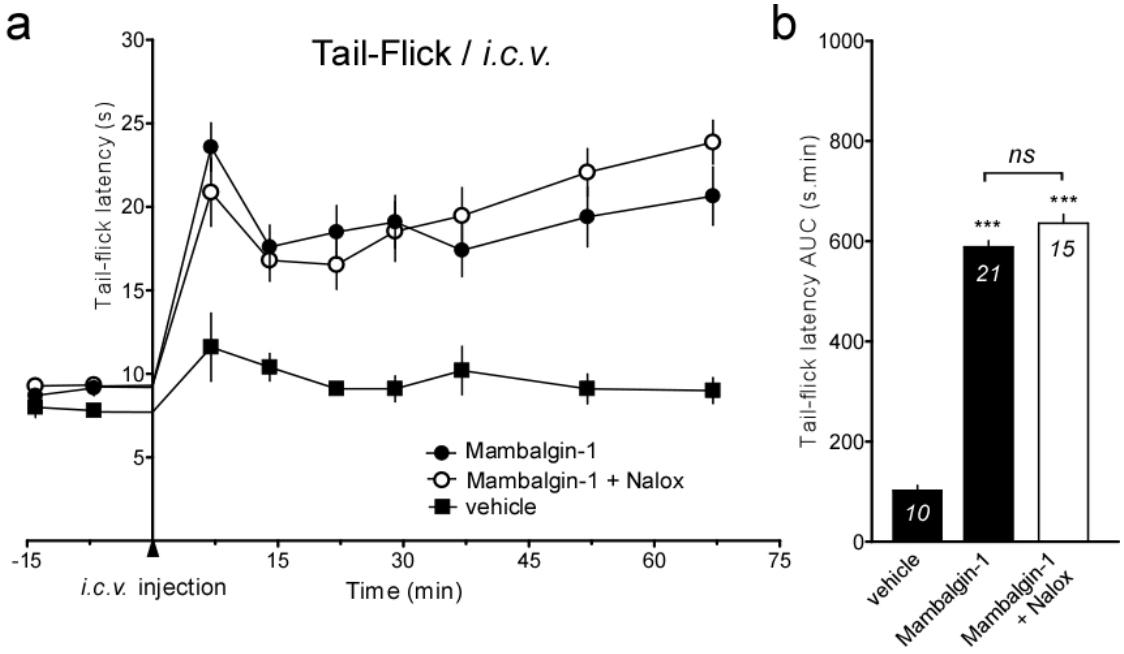

Supplementary Figure 8. Analgesic effect of intracerebroventricular injections of mambalgin-1 on acute thermal nociception.

a, Time-course of the effect of *i.c.v.* injection of mambalgin-1 (68 µM, 5 µl) on tail-flick latency (mean ± SEM, n=10-21). The naloxone sensitivity of the effect was assessed by *s.c.* injection of naloxone (Nalox, 2 mg kg^{-1}) ten minutes before the *i.c.v.* injection. **b**, Total analgesic effect calculated on each mouse as the Area Under Curve (AUC; s.min) (mean ± SEM, n=10-21). Comparison with vehicle unless specified. The *i.c.v.* injections were stereotaxically performed into the lateral ventricle of deeply anesthetized mice (1.5% isoflurane).

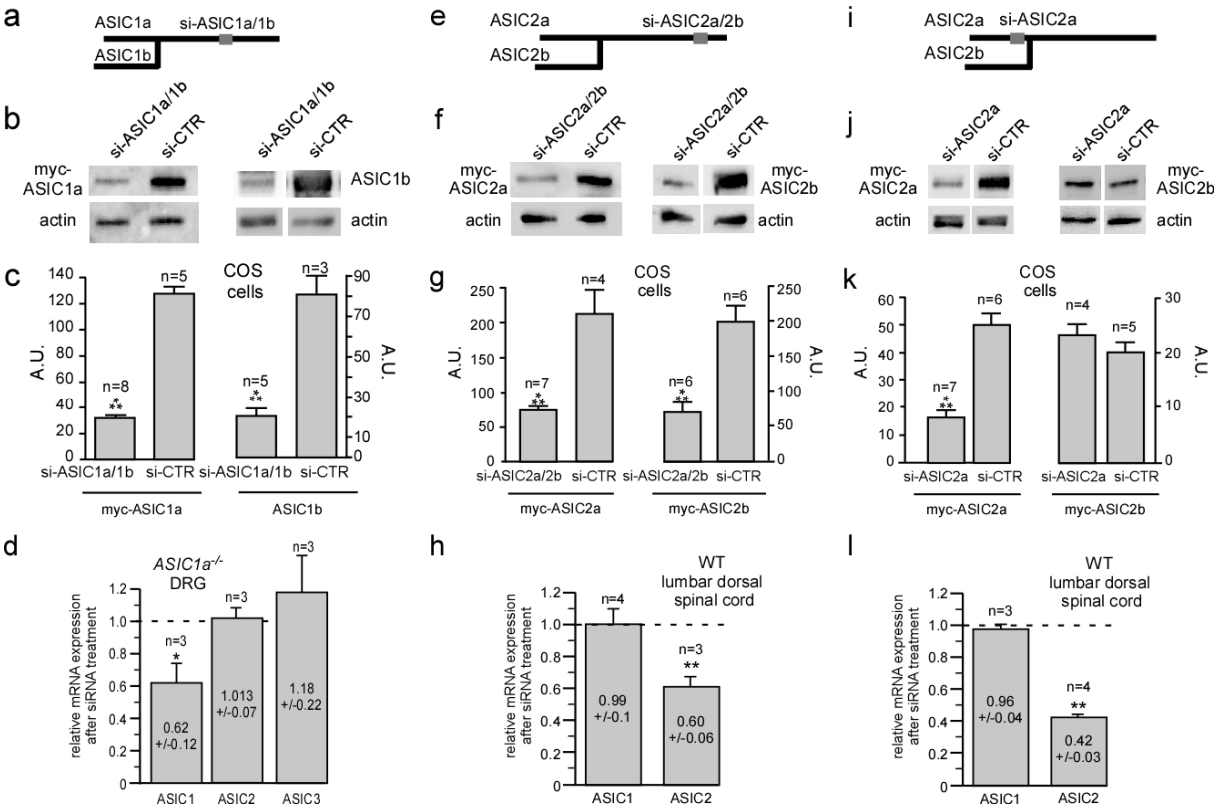

Supplementary Figure 9. *In vitro* and *in vivo* validation of the siRNAs targeting ASIC1a+1b, ASIC2a+2b and ASIC2a.

a-d, siRNA targeting both ASIC1a and ASIC1b (si-ASIC1a/1b) or control siRNA (si-CTR) were co-transfected in COS cells (25 nM) with a plasmid coding for myc tagged rat ASIC1a (myc-ASIC1a) or coding for rat ASIC1b. The level of protein was assessed 48h after transfection by Western blot with a myc antibody or an ASIC1-specific antibody (**b**). The blot was probed with an antibody against actin to demonstrate equal loading of proteins. A densitometric quantification of the signal shown in **b** has been done in **c** and showed a significant reduction of both ASIC1a and ASIC1b expression in COS-7 cells. *In vivo* siRNA treatment significantly reduced the level of ASIC1 transcripts in lumbar DRGs of *ASIC1a*$^{-/-}$ mice but did not affect the level of ASIC2 and ASIC3 transcripts (**d**). Since ASIC1a is lacking in these mice (the ASIC1a mRNA was not detected in similar experimental conditions), the decrease in ASIC1 expression represents the specific knockdown of ASIC1b in lumbar DRGs. **e-h**, similar experiments performed with a siRNA targeting both ASIC2a and ASIC2b (si-ASIC2a/2b), showing a significant knockdown of the expression of ASIC2a and ASIC2b in COS-7 cells (**f**,**g**). *In vivo* siRNA treatment against ASIC2 in wild-type mice significantly reduced the level of ASIC2 transcripts in the lumbar dorsal spinal cord but did not affect the level of ASIC1 transcripts (**h**). The ASIC3 mRNA was not detected in similar experimental

conditions. **i-l**, similar experiments performed with a siRNA targeting ASIC2a but not ASIC2b (si-ASIC2a), showing a significant knockdown of the expression of ASIC2a but no effect on the expression of ASIC2b in COS-7 cells (**j**,**k**). *In vivo* siRNA treatment against ASIC2a significantly reduced the level of ASIC2 transcripts in the lumbar dorsal spinal cord of wild-type mice but did not affect the level of ASIC1 transcripts (**l**), consistent with the fact that ASIC2a represents the predominant ASIC2 mRNA in the spinal cord [16].

A.U, arbitrary units. Mean ± S.E.M. **c**,**g**,**k,** *** : $p<0.001$ compared with si-CTR, unpaired *t*-test. **d**,**h**,**l,** *, $p<0.05$ and ** $p<0.01$, compared with ASIC2 and ASIC3 (**d**) or ASIC1 (**h**,**l**), paired *t*-test.

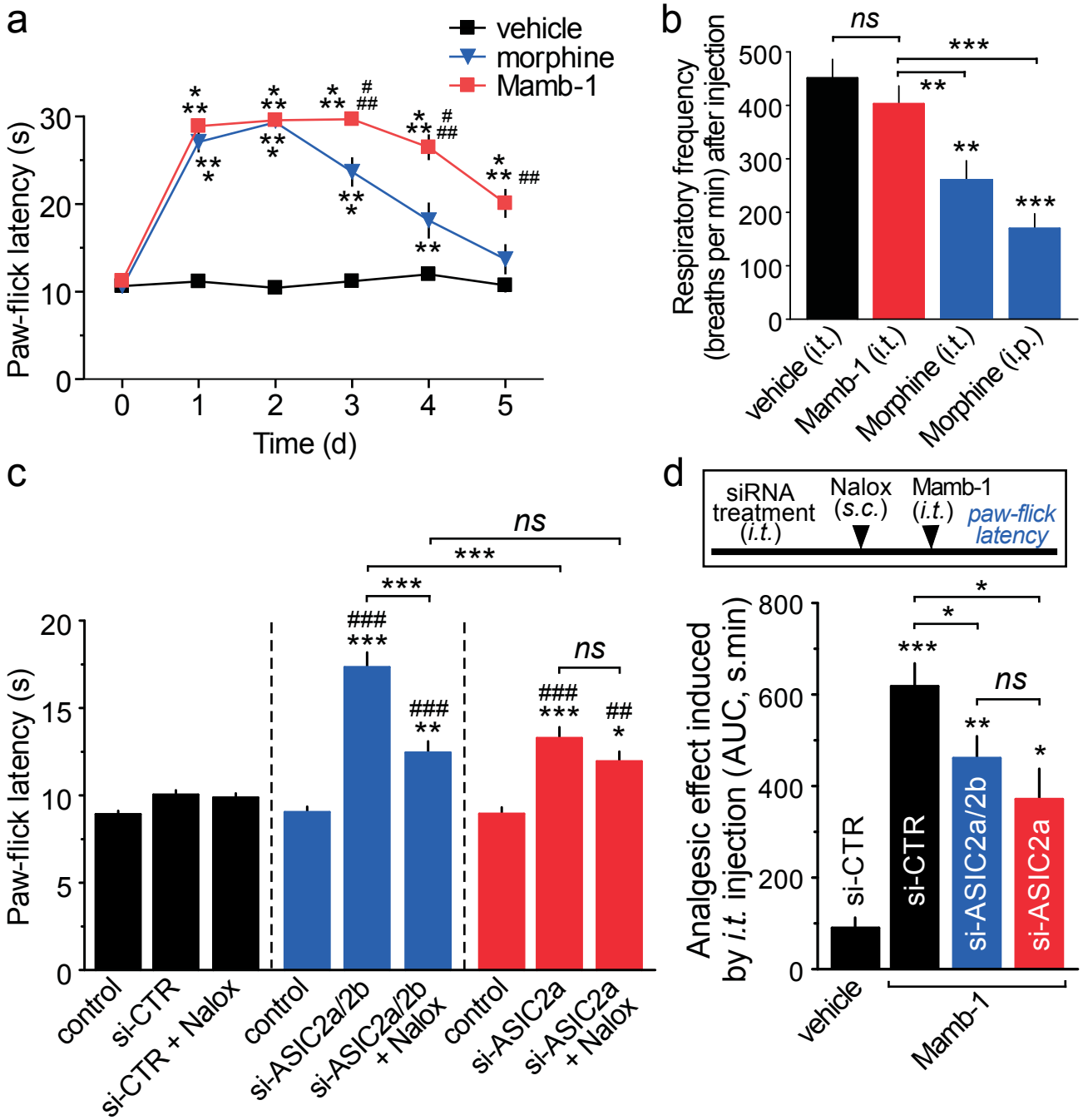
a
vehicle
morphine
Mamb-1
Paw-flick latency (s)
Time (d)
b
Respiratory frequency (breaths per min) after injection
ns
vehicle (i.t.)
Mamb-1 (i.t.)
Morphine (i.t.)
Morphine (i.p.)
c
Paw-flick latency (s)
control
si-CTR
si-CTR + Nalox
si-ASIC2a/2b
si-ASIC2a/2b + Nalox
si-ASIC2a
si-ASIC2a + Nalox
d
siRNA treatment (i.t.)
Nalox (s.c.)
Mamb-1 (i.t.)
paw-flick latency
Analgesic effect induced by i.t. injection (AUC, s.min)
si-CTR
si-ASIC2a/2b
si-ASIC2a
vehicle
Mamb-1

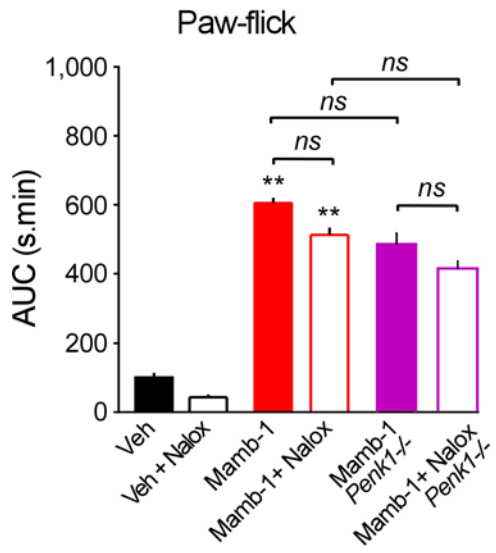

Supplementary Figure 10. Intrathecal injection of mambalgin-1 still produces a potent analgesia in mice deficient for the preproenkephalin gene. Effects on acute thermal pain (46°C) determined using the paw-immersion test showing a potent naloxone-insensitive analgesic effect in mice deficient for the preproenkephalin gene (*Penk1*$^{-/-}$, n=6), where the effect of PcTx1 was lost [5]. Area Under Curve (AUC) calculated from each mouse over the first 37 min. Data in WT mice shown for comparison are the same as in Fig. 2b. Naloxone (Nalox) was injected *s.c.* 10 minutes before *i.t* injection of the peptide. Mamb-1, mambalgin-1; Veh, vehicle, comparison with vehicle unless specified. Mean ± SEM.

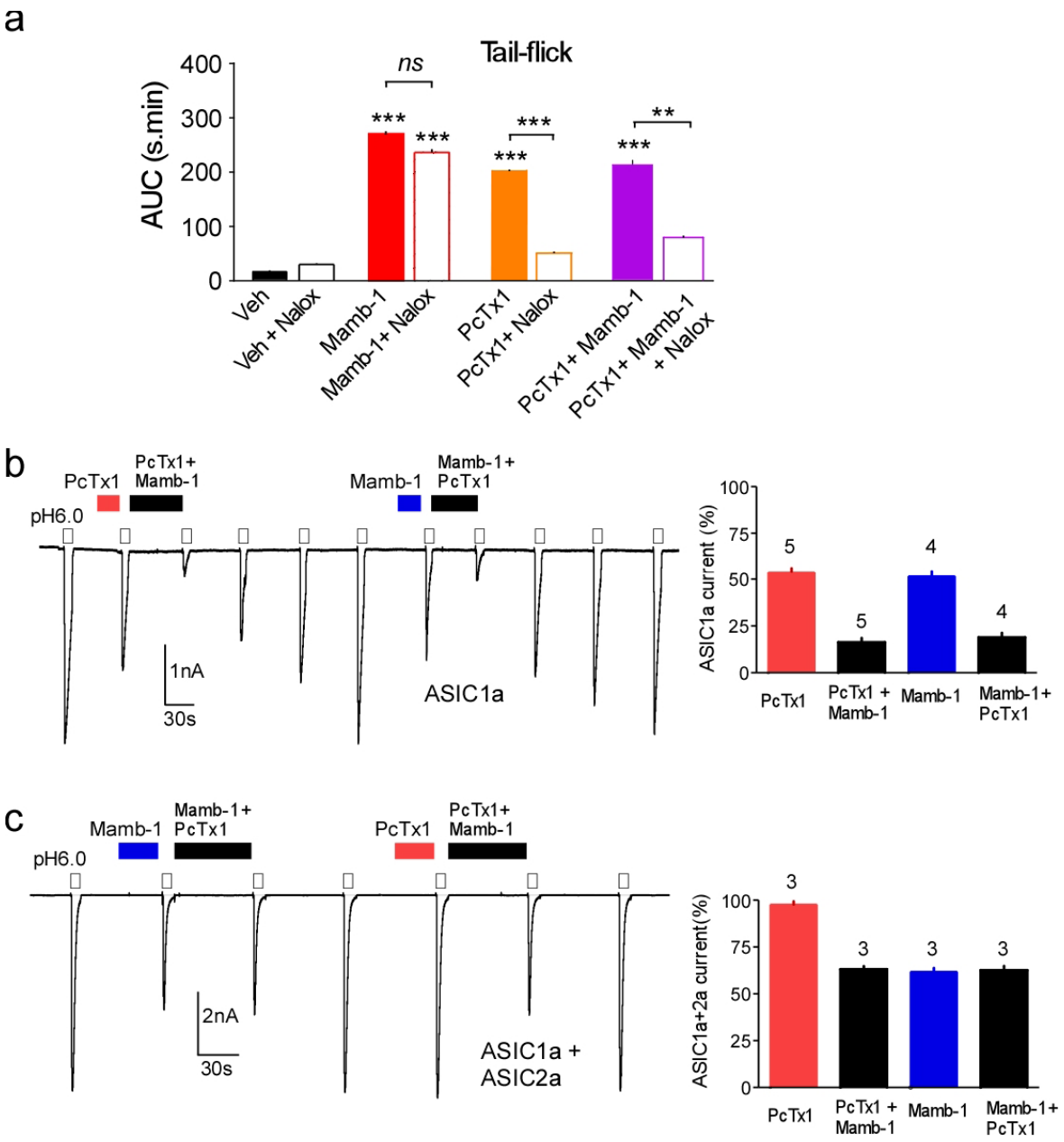

Supplementary Figure 11. Pain behavior experiments after central injection of mambalgin-1+PcTx1 and interaction between mambalgin-1 and PcTx1 on ASIC1a and ASIC1a+ASIC2a channels *in vitro*.

a, Effects on acute thermal pain (46°C) determined using the tail-immersion test showing a potent naloxone-sensitive analgesic effect similar to the effect of PcTx1 alone when mambalgin-1 (Mamb-1, 0.34 nmole) and PcTx1 (0.1 nmole) are intrathecally injected together (PcTx1 + Mamb-1, n=12-13). Data with vehicle, mambalgin-1 and PcTx1 alone are shown for comparison and are the same as in Fig. 2a. Area Under Curve (AUC) calculated from each mouse over the first 37 min. The opioid-dependent effect evoked by *i.t.* injection of PcTx1 is therefore dominant over the opioid-independent effect evoked by *i.t.* injection of

mambalgin-1. **b**, Lack of interaction between mambalgin-1 (Mamb-1) and PcTx1 on ASIC1a channels. ASIC1a currents stimulated by a pH drop from pH 7.4 to 6.0 show half-maximal inhibition by PcTx1 (1nM, *i.e.,* equivalent to IC_{50}) (46.0±4.9%, n=5), subsequent co-application of Mamb-1 (60nM, *i.e.,* equivalent to IC_{50}) + PcTx1 (1nM) induces additive inhibitory effect (83.7±4.9%, n=5). Similarly, a first application of Mamb-1 (60nM) inhibits ASIC1a (48.4 ±5.8%, n=4) and subsequent co-application of PcTx1 (1nM) + Mamb-1 (60nM) also induces an additive inhibitory effect (81.1±4.8%, n=4). **c**, Lack of interaction between mambalgin-1 (Mamb-1) and PcTx1 on ASIC1a+ASIC2a channels. ASIC1a+ASIC2a currents evoked by a pH drop from pH 7.4 to 6.0 are half-inhibited by Mamb-1 (300nM, *i.e.,* equivalent to IC_{50}) (38.1±4.9%, n=3) but subsequent application of PcTx1 (10nM) has no additional effect (37.4±3.3%, n=3). Inversely, application of PcTx1 (10nM) does not inhibit ASIC1a+ASIC2a (2.3±2.3%, n=3), as also shown in Supplementary Figure 3c and in previous work [14], while subsequent application of PcTx1 (10 nM) + Mamb-1 (300nM) blocks the current (36.9±2.9%, n=3). Holding potential -60 mV. **b, c,** Original currents traces (left panel) and mean ± SEM (right panel).

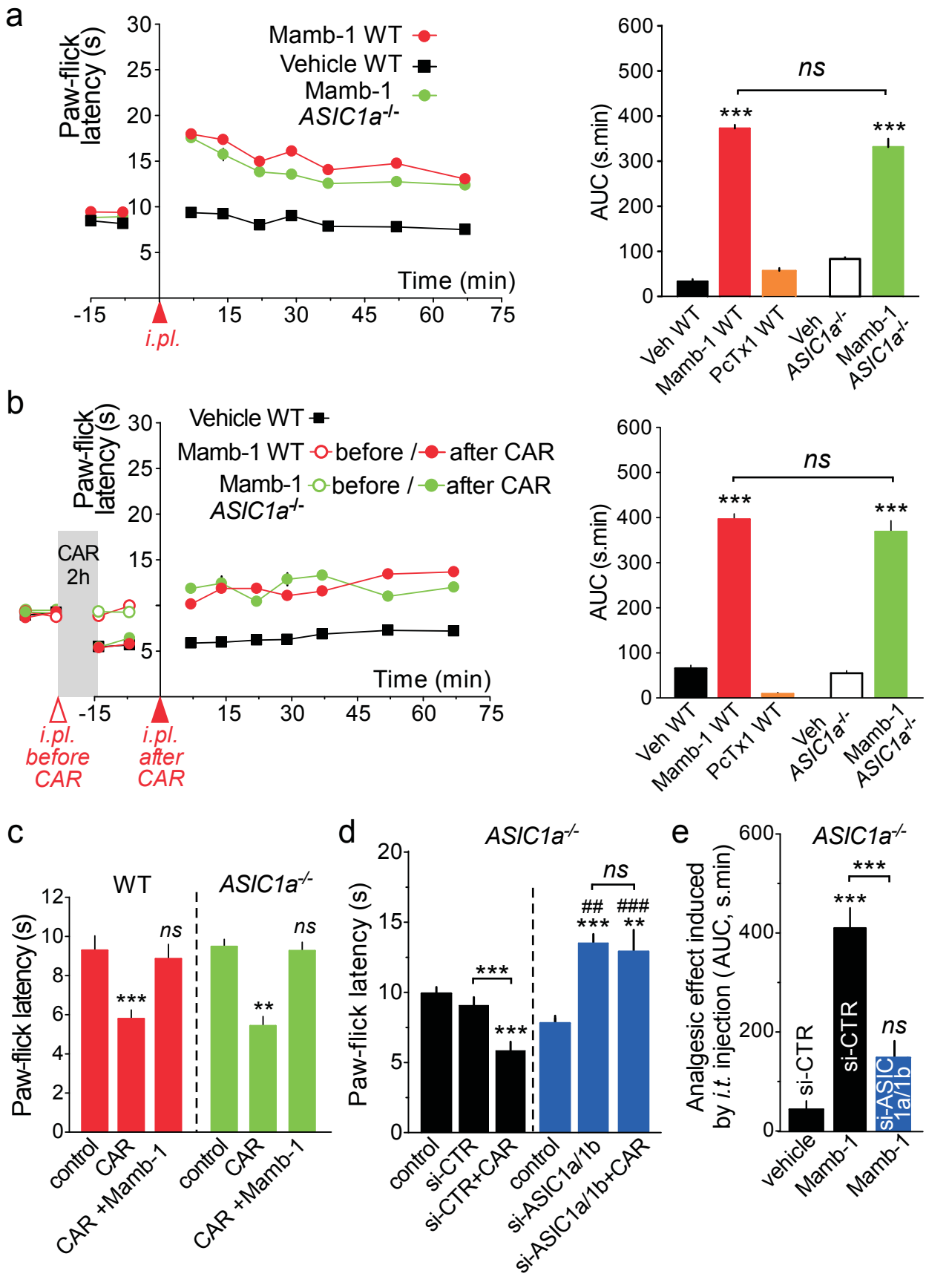
a
Paw-flick latency (s)
Mamb-1 WT
Vehicle WT
Mamb-1 ASIC1a-/-
Time (min)
i.pl.
AUC (s.min)
ns
***
Veh WT
Mamb-1 WT
PcTx1 WT
Veh ASIC1a-/-
Mamb-1 ASIC1a-/-
b
Vehicle WT
Mamb-1 WT before / after CAR
Mamb-1 ASIC1a-/- before / after CAR
CAR 2h
i.pl. before CAR
i.pl. after CAR
c
WT
ASIC1a-/-
control
CAR
CAR +Mamb-1
d
si-CTR
si-CTR+CAR
si-ASIC1a/1b
si-ASIC1a/1b+CAR
##
###
e
Analgesic effect induced by i.t. injection (AUC, s.min)
vehicle
Mamb-1
si-CTR
si-ASIC 1a/1b

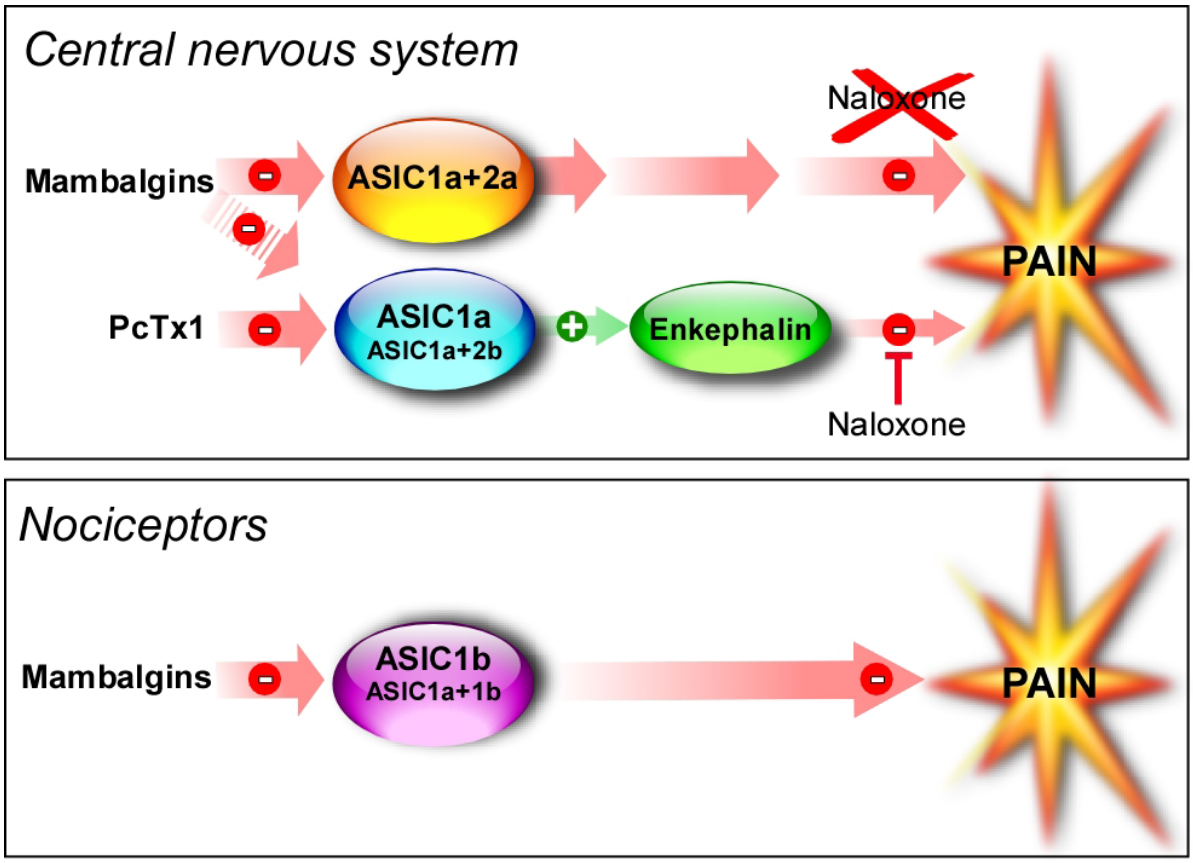

Supplementary Figure 12. Mambalgins have analgesic effects by targeting both central neurons and primary nociceptors, but through different ASIC subtypes.

Mambalgins are able to block all the ASIC channel subtypes expressed in the central nervous system (*i.e.*, ASIC1a, ASIC1a+ASIC2b and ASIC1a+ASIC2a) but the peptides essentially evoke a naloxone-independent effect upon central injection. This suggests that *in vivo* and at the concentration that has been used, mambalgins only efficiently target the opioid-independent pain pathway involving ASIC1a+ASIC2a channels, but not the opioid-dependent pathway previously associated with ASIC1a and probably ASIC1a+ASIC2b channels and targeted by PcTx1. This is consistent with the fact that the opioid-dependent pathway prevails when PcTx1 and mambalgins are centrally injected together (see supplementary Figure 11). In nociceptors, ASIC1b-containing channels, but not ASIC1a, are targeted by mambalgins to evoke analgesia, demonstrating a role for ASIC1b in triggering cutaneous pain.

Supplementary References

44. King, G.F., Gentz, M.C., Escoubas, P. & Nicholson, G.M. A rational nomenclature for naming peptide toxins from spiders and other venomous animals. *Toxicon* **52**, 264-276 (2008).
45. Joubert, F.J. Snake venom toxins. The amino acid sequences of two toxins (CM-2a and CM-3) from Naja haje annulifera (Egyptian cobra) venom. *Hoppe Seylers Z Physiol Chem* **358**, 377-390 (1977).
46. Joubert, F.J. & Taljaard, N. The complete primary structure of toxin CM-1b from Hemachatus haemachatus (Ringhals) snake venom. *Toxicon* **18**, 191-198 (1980).
47. He, Y.Y., Lee, W.H. & Zhang, Y. Cloning and purification of alpha-neurotoxins from king cobra (Ophiophagus hannah). *Toxicon* **44**, 295-303 (2004).
48. Lou, X.*, et al.* The atomic resolution crystal structure of atratoxin determined by single wavelength anomalous diffraction phasing. *J Biol Chem* **279**, 39094-39104 (2004).
49. Bilwes, A., Rees, B., Moras, D., Menez, R. & Menez, A. X-ray structure at 1.55 A of toxin gamma, a cardiotoxin from Naja nigricollis venom. Crystal packing reveals a model for insertion into membranes. *J Mol Biol* **239**, 122-136 (1994).
50. Chen, T.S.*, et al.* Structural difference between group I and group II cobra cardiotoxins: X-ray, NMR, and CD analysis of the effect of cis-proline conformation on three-fingered toxins. *Biochemistry* **44**, 7414-7426 (2005).
51. Singhal, A.K., Chien, K.Y., Wu, W.G. & Rule, G.S. Solution structure of cardiotoxin V from Naja naja atra. *Biochemistry* **32**, 8036-8044 (1993).
52. Gaucher, J.F., Menez, R., Arnoux, B., Pusset, J. & Ducruix, A. High resolution x-ray analysis of two mutants of a curaremimetic snake toxin. *Eur J Biochem* **267**, 1323-1329 (2000).
53. Rustay, N.R., Wahlsten, D. & Crabbe, J.C. Influence of task parameters on rotarod performance and sensitivity to ethanol in mice. *Behav Brain Res* **141**, 237-249 (2003).